approach in a human neuroglioma model. We found that cysteine protease inhibitor E-64d (12) and cathepsin B-specific inhibitor CA-074Me (12–15) could cause the accumulation of both CTFs and AICD with no change in α-, β-, and γ-secretase activities. Moreover, we found that γ-secretase prefers phosphorylated CTFs on Thr668 (at a position corresponding to the APP_{695} isoform), whereas cathepsin B catalyzed degradation of CTFs regardless of phosphorylation. Altogether, our results suggest that cathepsin B plays novel roles in the metabolism of the APP C-terminal region and that inhibition of APP phosphorylation is an attractive therapeutic target for AD.

MATERIALS AND METHODS

Reagents

CA-074 (also known as cathepsin B inhibitor III; [L-3-*trans*-(propylcarbamoyl)oxirane-2-carbonyl]-L-isoleucyl-L-proline), CA-074Me (also known as cathepsin B inhibitor IV; [L-3-*trans*-(propylcarbamoyl)oxirane-2-carbonyl]-L-isoleucyl-L-proline methyl ester), E-64d [(L-3-*trans*-ethoxycarbonyloxirane-2-carbonyl)-L-leucine (3-methylbutyl) amide], lactacystine ([*N*-acetyl-*S*-{(2*R*,3*S*,4*R*)-3-hydroxy-2-[(1*S*)-1-hydroxy-2-methylpropyl]-4-methyl-5-oxo-2-pyrrolidinecarbonyl}-L-cysteine), DAPT [also known as γ-secretase inhibitor IX; (3,5-difluorophenylacetyl)-L-alanyl-L-2-phenylglycine *t*-butyl ester], and L-685,458 (also known as γ-secretase inhibitor X; [(2*R*,4*R*,5*S*)-2-benzyl-5-(*t*-butyloxycarbonylamino)-4-hydroxy-6-phenylhexanoyl]-L-leucyl-L-phenylalanine amide) were purchased from the Peptide Institute (Osaka, Japan). β-Secretase inhibitor IV (*N*-[(1*S*, 2*R*)-1-benzyl-3-(cyclopropylamino)-2-hydroxypropyl]-5-[methyl(methylsulfonyl)amino-*N*'-[(1*R*)-1-phenylethyl]isophthalamide), compound E (also known as γ-secretase inhibitor XXI; (*S*,*S*)-2-[2-(3,5-difluorophenyl)-acetylamino]-*N*-(1-methyl-2-oxo-5-phenyl-2,3-dihydro-1H-benzo[e] [1,4]diazepin-3-yl)-propionamide), and cathepsin G inhibitor I ([2-[3-[(1-benzoylpiperidin-4-yl)-methylcarbamoyl] naphthalen-2-yl]-1-naphthalen-1-yl-2-oxoethyl]phosphonic acid) were purchased from Merck KGaA (Darmstadt, Germany). Pepstatin A, chloroquine, and NH_4Cl were obtained from Sigma-Aldrich Co. (St. Louis, MO, USA). Chloroquine was dissolved in sterilized PBS, and all other powdered reagents were dissolved in sterilized dimethyl sulfoxide (DMSO) and added into the cell culture medium to yield 0.2% DMSO as a final concentration.

Cell culture

A murine neuroblastoma Neuro2a (N2a) cell line ($mNotch^{\Delta E}$-N2a cells) stably expressing both mouse Notch-deleted extracellular domain with myc tag ($mNotch^{\Delta E}$) and enhanced green fluorescent protein (16), a human neuroglioma H4 cell line stably expressing human APP_{695} with the Swedish mutation (APP_{NL}-H4 cells) (17) or stably expressing human APP_{695} with the Swedish mutation and a point mutation at a phosphorylation site [Thr to Ala on 668 (APP_{695} numbering); APP_{NL_TA}-H4 cells], and mouse embryonic fibroblast cells with deficiencies of both *PS1* and *PS2* genes ($PS1^{-/-}PS2^{-/-}$ cells) (18) were cultured in DMEM (Invitrogen, Carlsbad, CA, USA) at 37°C in 5% CO_2. The DMEM was supplemented with 10% FBS (Invitrogen), 100 U/ml penicillin, and 100 μg/ml streptomycin (Invitrogen). In addition, G418 (Merck) was supplemented for $mNotch^{\Delta E}$-N2a cells (160 μg/ml) and $PS1^{-/-}PS2^{-/-}$ cells (200 μg/ml), and hygromycin B (Wako Pure Chemicals Industries, Osaka, Japan) was supplemented for APP_{NL}-H4 cells (150 μg/ml) and APP_{NL_TA}-H4 cells (225 μg/ml). After passage by trypsinization, cells were grown for 24–36 h and then treated with reagents: CA-074Me (0.1, 1, or 10 μM), pepstatin A (10 μM), cathepsin G inhibitor I (10 μM), E-64d (10 μM), compound E (1 μM), DAPT (1 μM), L-685,458 (1 μM), β-secretase inhibitor IV (1 μM), lactacystin (1 μM), chloroquine (1 μM), or NH_4Cl (1 mM), for the indicated time.

Sample preparation for Western blot analysis

Cells treated with reagents were harvested and lysed in a buffer containing 10 mM HEPES (pH 7.4), 150 mM NaCl, 0.5% Triton X-100, and protease inhibitor cocktail (Roche Diagnostics, Mannheim, Germany) on ice. The cell lysate was freeze-thawed at three 20-min intervals and centrifuged at 13,000 *g* for 15 min at 4°C. The supernatant protein concentrations were determined using a BCA protein assay kit (Pierce Biotechnology, Rockford, IL, USA). sAPP secreted into the conditioned medium was precipitated with heparin agarose resin (Pierce Biotechnology), as described previously (16).

Western blot analysis

Equal amounts of proteins from the cell lysates or sAPP collected from the equal volumes of the conditioned medium were subjected to SDS-PAGE, and proteins in the gels were transferred to PVDF membranes (Hybond-P; GE Healthcare, Little Chalfont, UK) or nitrocellulose transfer membranes (Protran; Whatman, Dassel, Germany). The membranes were probed with an appropriate primary antibody and then reacted with an appropriate secondary antibody, specifically horseradish peroxidase-conjugated anti-mouse or anti-rabbit IgG (GE Healthcare). The protein band was visualized using an enhanced chemiluminescence (ECL) detection method (GE Healthcare), and band intensity was analyzed with a densitometer (LAS-4000; GE Healthcare), using Science Laboratory 2001 Image Gauge software (GE Healthcare).

Monoclonal antibody 2B3 (Immuno-Biological Laboratories, Gunma, Japan), which recognizes amino acid residues at the C terminus of human sAPPα, was used at a concentration of 2 μg/ml to detect sAPPα (anti-sAPPα antibody). Polyclonal anti-$sAPP\beta_{NL}$ antibody was used at a concentration of 1:1000 to detect $sAPP\beta_{NL}$ (APP with Swedish mutation), as described previously (17). Monoclonal antibody 82E1 (Immuno-Biological Laboratories), which recognizes amino acid residues 1–16 of the human Aβ sequence, was used at a concentration of 1 μg/ml to detect Aβ (anti-Aβ antibody). Polyclonal anti-APP antibody (catalog no. A8717; Sigma-Aldrich), which recognizes amino acid residues 676–695 at the C terminus of the APP_{695} isoform, was used at a concentration of 1:15,000 to detect full-length APP (FL-APP), CTFs, and AICD (anti-APP antibody). Polyclonal anti-phosphorylated APP antibody (Cell Signaling Technology, Danvers, MA, USA), which recognizes the phosphorylation of Thr668, was used at a concentration of 1:1000. Monoclonal antibody AC-74 (Sigma-Aldrich), which recognizes amino acid residues at the N-terminal end of β-actin, was used at a concentration of 1:5000. Monoclonal antibody 9B11 (Cell Signaling Technology), which recognizes the myc epitope tag corresponding to amino acid residues 410–419 of human c-Myc, was used at a concentration of 1:1000.

Cell-free assay

The microsomal fraction was isolated from APP_{NL}-H4 cells, as described previously (8). Briefly, harvested APP_{NL}-H4 cells

were homogenized in buffer A (20 mM PIPES, pH 7.0; 140 mM KCl; 0.25 M sucrose; and 5 mM EGTA), and the homogenates were then centrifuged at 800 *g* for 10 min to remove nuclei and cell debris. The resultant supernatants were centrifuged at 100,000 *g* for 1 h. The pellets were suspended in buffer A and centrifuged again. The resultant pellets were suspended in buffer A containing various protease inhibitors, including 50 μM diisopropyl fluorophosphate (Wako), 50 μM phenylmethylsulfonyl fluoride (Sigma-Aldrich), 0.1 μg/ml N^{α}-*p*-tosyl-L-lysine chloromethyl ketone (Sigma-Aldrich), 0.1 μg/ml antipain (Peptide Institute), 0.1 μg/ml leupeptin (Peptide Institute), 100 μM EGTA (Wako), 1 mM thiorphan (Sigma-Aldrich), and 5 mM phenanthroline (Nacalai Tesque, Kyoto, Japan), for a final concentration of 2.5 mg protein/ml. The mixtures were incubated at 37°C for 1 h with CA-074, CA-074Me, or L-685,458. The reaction was terminated using a solution of chloroform:methanol (2:1). After extracting lipids with chloroform:methanol:water solution (1:2:0.8), the protein fractions were separated on conventional 16.5% Tris/Tricine gels to detect Aβ or AICD product by Western blot analysis.

In vitro degradation assay

In vitro cleavage of AICD was performed in 30 μl of 100 mM sodium acetate buffer (pH 5.5), containing 1 mM EDTA and 8 mM cysteine with or without synthetic AICD (Merck). Various amounts of purified cathepsin B from human liver (Merck) were added with or without 1 μM CA-074. The mixtures were incubated at 37°C for the indicated time, and sample buffer was then added to stop the reaction. The products were analyzed by Western blotting conventional 16.5% Tris/Tricine gels with an anti-APP antibody.

Statistical analysis

All values are expressed as means ± SE. For comparisons of 2 groups, a 2-tailed Student's *t* test was used. For comparisons among >3 groups, a Dunnett's or Student-Newman-Keul multiple comparison test was used. Differences were considered significant at values of $P < 0.05$.

RESULTS

Cathepsin B inhibitors, CA-074Me and E-64d, lead to the accumulation of CTFs and AICD with no change in α- and β-secretase activities

Weak bases, such as chloroquine or NH_4Cl, alkalize the intracellular pH of acidic compartments (19, 20). If there are proteases responsible for the degradation of CTFs and AICD other than γ-secretase, we should be able to detect the accumulation of CTFs by treatment with chloroquine or NH_4Cl in γ-secretase-deficient cells. To verify this hypothesis, we treated *PS1*$^{-/-}$ *PS2*$^{-/-}$ cells and APP_{NL}-H4 cells with chloroquine or NH_4Cl (**Fig. 1*A*, *B***). After chloroquine or NH_4Cl treatment, accumulation of CTFα was observed in *PS1*$^{-/-}$ *PS2*$^{-/-}$ cells (Fig. 1*A*). We were unable to detect CTFβ, which is derived from endogenous APP, likely due to the low β-secretase activity in these cells (Fig. 1*A*). In chloroquine- or NH_4Cl-treated APP_{NL}-H4 cells, we also observed accumulation of both CTFα and AICD with no change in FL-APP (Fig. 1*B*). Conversely, treatment with the γ-secretase inhibitor L-685,458 produced a significant accumulation of CTFs and lower production of AICD in APP_{NL}-H4 cells (Fig. 1*B*).

To address whether the cathepsin family is involved in degrading CTFs and AICD, we treated APP_{NL}-H4 cells with representative cathepsin inhibitors (Fig. 1*C*, *D*). Cathepsins B, D, and G are cysteine, aspartyl, and serine proteases, respectively. E-64d generally inhibits cysteine proteases. Western blot analysis showed that CTFα, CTFβ, and AICD did not significantly accumulate in the presence of inhibitors for cathepsins G and D (cathepsin G inhibitor I and pepstatin A, respectively), but E-64d and the cathepsin B-specific inhibitor CA-074Me markedly increased accumulation of CTFα, CTFβ, and AICD (Fig. 1*C*). In addition, treatment with the proteasome inhibitor lactacystin exerted no significant influence on the levels of CTFα, CTFβ, and AICD production (Fig. 1*C*). It has been reported that cathepsin B prefers wild-type APP (APP_{WT}) to APP_{NL} (12). Although CA-074Me treatment led to significant accumulation of CTFα, CTFβ, and AICD in stably APP_{WT}-overexpressing H4 cells (APP_{WT}-H4 cells), this efficacy in APP_{WT}-H4 cells was less than that observed in APP_{NL}-H4 cells (Supplemental Fig. S1).

If CA-074Me causes up-regulation of both α- and β-secretase activities, CTFα and CTFβ might simultaneously accumulate in cells. To evaluate the effects of CA-074Me on α- and β-secretase activities, sAPPα and sAPPβ levels were assessed in the conditioned medium from APP_{NL}-H4 cells treated with CA-074Me (Fig. 1*E*, *F*). No change in either sAPPα or sAPPβ levels was observed (Fig. 1*F*). Therefore, we concluded that cysteine protease cathepsin B was a major CTF- and AICD-degrading enzyme with no effect on α- and β-secretase activities.

Time course and dose dependency of the accumulation of CTFs and AICD *via* cathepsin B inhibition

To accurately assess the drug efficacy of CA-074Me, we performed time-course and dose-dependency analyses in APP_{NL}-H4 cells (**Fig. 2**). Time-course analysis revealed that CA-074Me treatment for 6 h or longer resulted in the gradual accumulation of CTFα, CTFβ, and AICD, as compared to 0 h of treatment (Fig. 2*A*, *B*). The effect of CA-074Me was observed to differ among CTFα, CTFβ, CTFs, and AICD. The accumulation of CTFα, CTFβ, and CTFs reached a peak at 12 h; in contrast, an accumulation of AICD showed a monotonic increase over a 0- to 24-h period (Fig. 2*A*, *B*). Dose-dependency analysis demonstrated that inhibition of cathepsin B by CA-074Me at 1 μM or more led to a significant accumulation of CTFα, CTFβ, CTFs, and AICD (Fig. 2*C*, *D*).

CA-074 and CA-074Me have no inhibitory effect on γ-secretase activity of the presenilin complex

Several drugs have been reported to inhibit or modulate γ-secretase activity, and nonsteroidal anti-inflammatory

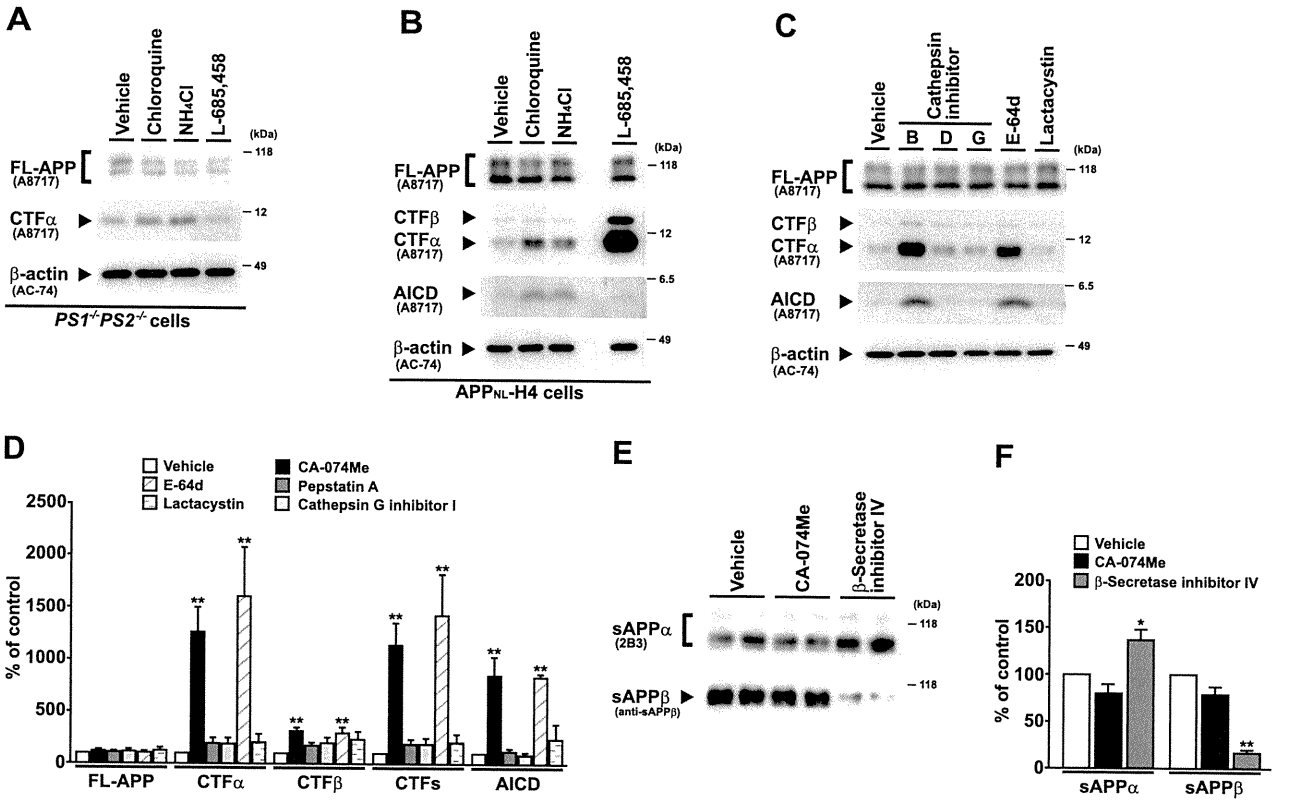

Figure 1. CA-074Me and E-64d lead to the accumulation of CTFs and AICD with no change in α- and β-secretase activities. *A*) Representative Western blots show the effect of treatment with chloroquine (1 μM), ammonium chloride (1 mM), or L-685,458 (1 μM) for 24 h on FL-APP, and CTFα levels in $PS1^{-/-}PS2^{-/-}$ cells. FL-APP and CTFα were detected with A8717; β-actin was detected with AC-74. *B*) Representative Western blots show the effect of treatment with chloroquine (1 μM), ammonium chloride (1 mM), or L-685,458 (1 μM) for 24 h on FL-APP, CTFα, CTFβ, and AICD levels in APP_{NL}-H4 cells. FL-APP, CTFα, CTFβ, and AICD were detected with A8717; β-actin was detected with AC-74. *C*) Amounts of FL-APP, CTFα, CTFβ, and AICD in the cell lysates of APP_{NL}-H4 cells treated with cathepsin inhibitors [B, CA-074Me (10 μM); D, pepstatin A (10 μM); G, cathepsin G inhibitor I (10 μM)], E-64d (10 μM), or lactacystin (1 μM) for 24 h were measured by semiquantitative Western blot analysis. β-Actin was used as loading control (*A–C*). *D*) Results of Western blot analysis shown in *C*. Data represent means ± SE of 5 experiments. $^{**}P < 0.01$: significantly different from the vehicle-treated group. *E*) Amounts of sAPPα or sAPPβ in conditioned medium from APP_{NL}-H4 cells treated with CA-074Me (10 μM) or β-secretase inhibitor IV (1 μM; as a positive control) for 24 h were measured by semiquantitative Western blot analysis with 2B3 or anti-sAPPβ antibody, respectively. *F*) Results of Western blot analysis shown in *E*. Data represent means ± SE of 4 experiments. $^{*}P < 0.05$, $^{**}P < 0.01$ *vs.* vehicle-treated group.

drugs (NSAIDs) are representative γ-secretase modulators that lower Aβ42 production and increase Aβ38 production. To elucidate the effects of CA-074Me on γ-secretase activity, we examined whether CA-074Me has a direct effect on γ-secretase activity (**Fig. 3**). We prepared a total cell membrane fraction of APP_{NL}-H4 cells and incubated this fraction with L-685,458, CA-074Me, or CA-074, which is a nonmethyl esterified analog of CA-074Me. Western blot analysis with anti-APP antibody showed that a γ-secretase inhibitor significantly suppressed production of AICD (Fig. 3*A*, lane 8; *B*). Treatment with cathepsin B-specific inhibitors CA-074 or CA-074Me did not suppress γ-secretase activity in the membrane fraction, as compared to treatment with vehicle (Fig. 3*A*, lane 3 *vs.* 4–7; *B*). Similarly, Western blot analysis with the antibody 82E1 showed that both CA-074 and CA-074Me failed to block production of Aβ (Fig. 3*C*, lane 3 *vs.* lanes 4–7, *D*). However, L-685,458 inhibited γ-secretase activity, leading to a decrease in Aβ levels, as compared to vehicle (Fig. 3*C*, lane 8; *D*). A weak band (Fig. 3*C*, lane 8) is believed to be Aβ preexisting in the membrane fraction (Fig. 3*C*, lane 2, bottom band of Aβ), and new Aβ was processed from longer Aβ (Fig. 3*C*, lane 2, top band of Aβ). This observation is consistent with a previous report that suggests longer Aβ can be processed to shorter Aβ by γ-secretase in the presence of L-685,458 without production of AICD (21). These results clearly demonstrate that the cathepsin B-specific inhibitors CA-074 and CA-074Me did not significantly affect the activity of γ-secretase.

Inhibition of cathepsin B has no inhibitory effect on Notch processing

With a rare exception, all γ-secretase substrates are membrane-associated stubs, which are type I membrane proteins with ectodomain shedding. The intracellular domain of several γ-secretase substrates cleaved by γ-secretase translocates into the nucleus, and this domain has been shown to activate transcription. To assess the effect of CA-074Me on the processing of Notch, another γ-secretase substrate, we treated $mNotch^{\Delta E}$-

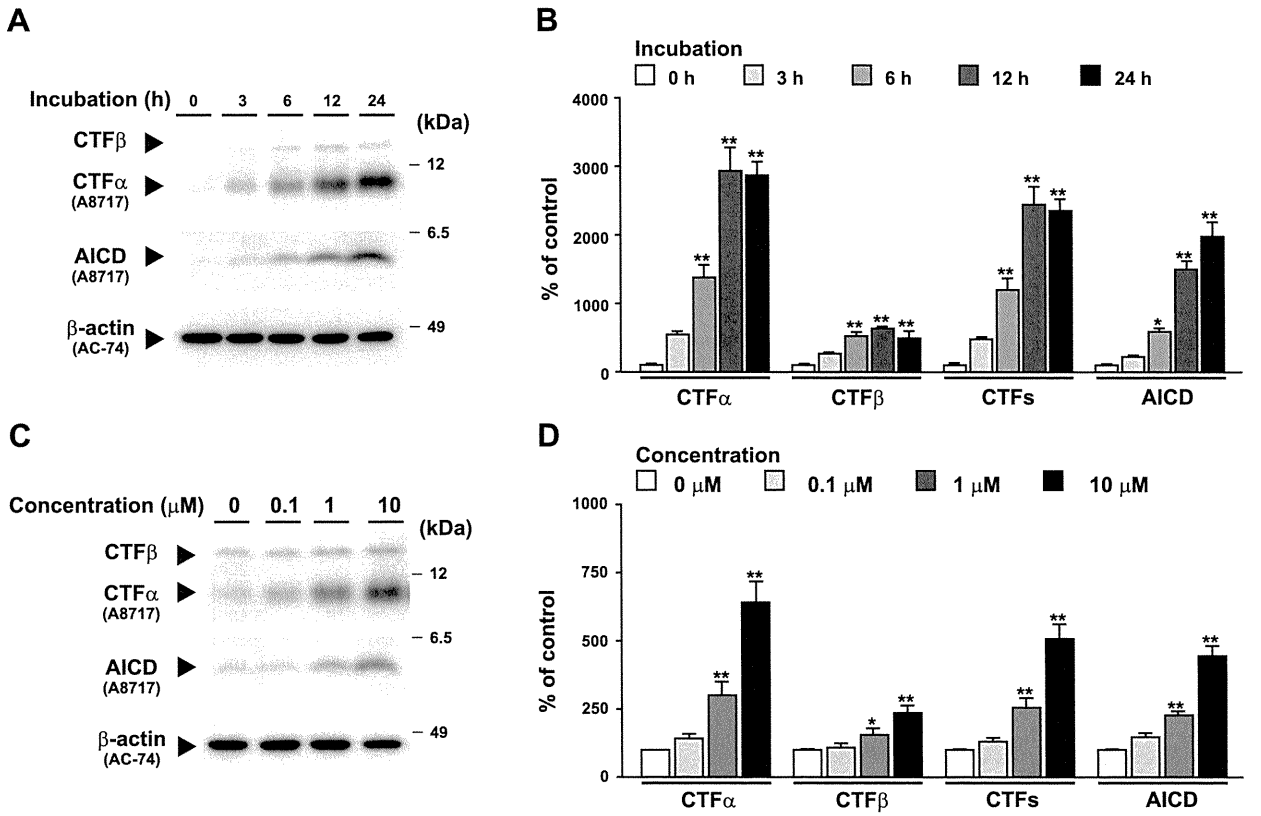

Figure 2. Inhibition of cathepsin B leads to the time- and dose-dependent accumulation of CTFs and AICD. *A*) Amounts of CTFα, CTFβ, and AICD in the cell lysates of APP_{NL}-H4 cells treated with CA-074Me (10 μM) for 0, 3, 6, 12, or 24 h were measured by semiquantitative Western blot analysis with A8717. *B*) Results of Western blot analysis shown in *A*. *C*) Amounts of CTFα, CTFβ, and AICD in the cell lysates of APP_{NL}-H4 cells treated with CA-074Me (0, 0.1, 1, or 10 μM) for 24 h were measured by semiquantitative Western blot analysis with A8717. *D*) Results of Western blot analysis shown in *C*. β-Actin was used as loading control and detected with AC-74 (*A*, *C*). Data represent means ± SE of 4 experiments. $*P < 0.05$, $**P < 0.01$ *vs.* control treatment group.

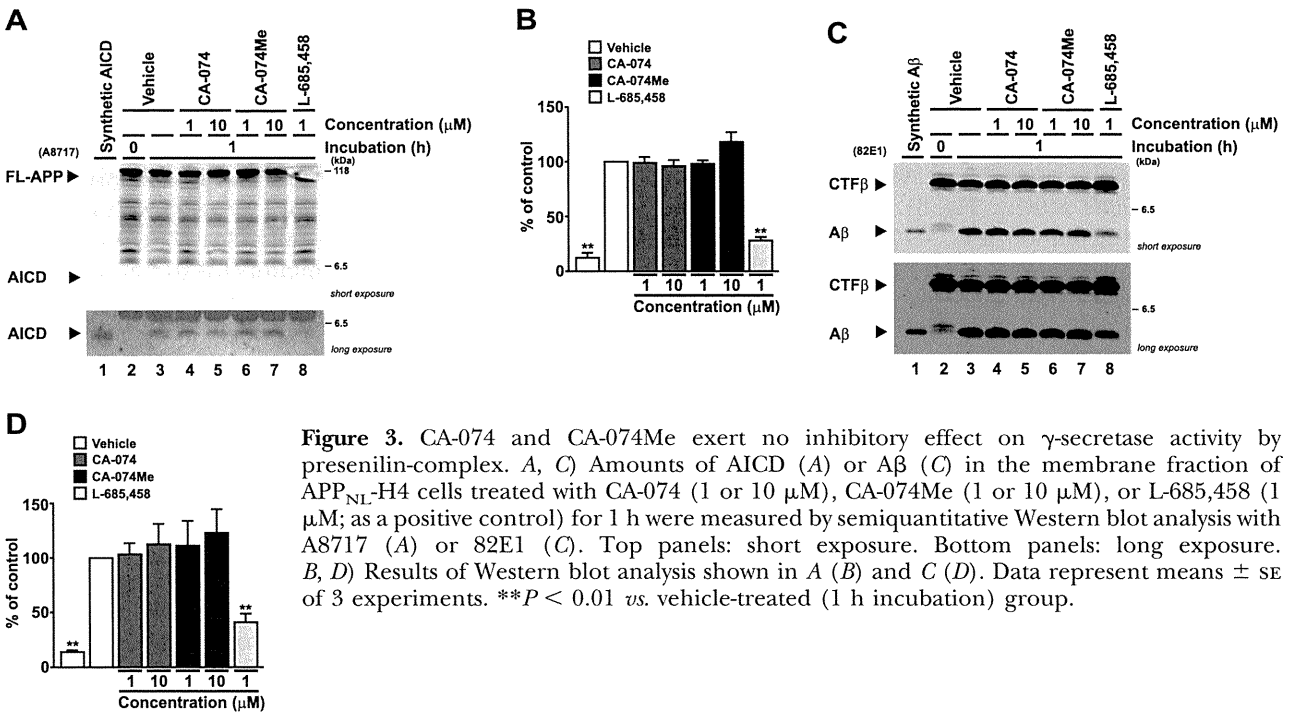

Figure 3. CA-074 and CA-074Me exert no inhibitory effect on γ-secretase activity by presenilin-complex. *A*, *C*) Amounts of AICD (*A*) or Aβ (*C*) in the membrane fraction of APP_{NL}-H4 cells treated with CA-074 (1 or 10 μM), CA-074Me (1 or 10 μM), or L-685,458 (1 μM; as a positive control) for 1 h were measured by semiquantitative Western blot analysis with A8717 (*A*) or 82E1 (*C*). Top panels: short exposure. Bottom panels: long exposure. *B*, *D*) Results of Western blot analysis shown in *A* (*B*) and *C* (*D*). Data represent means ± SE of 3 experiments. $**P < 0.01$ *vs.* vehicle-treated (1 h incubation) group.

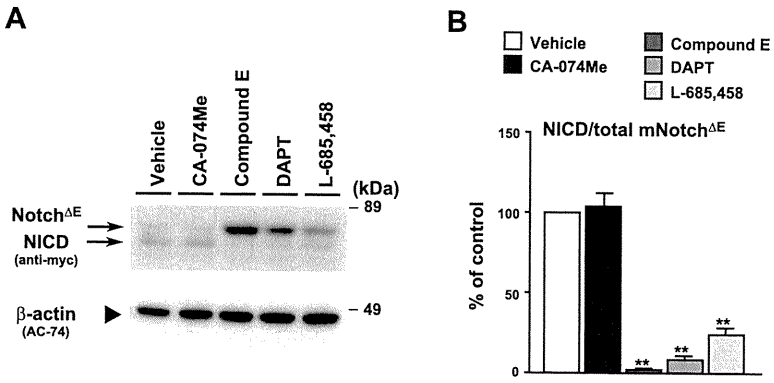

Figure 4. Inhibition of cathepsin B has no inhibitory effect on Notch processing. *A*) Amounts of Notch fragments in the cell lysates of mNotch$^{\Delta E}$-N2a cells treated with CA-074Me (10 μM) or γ-secretase inhibitors (compound E, DAPT, and L-685,458; 1 μM) for 24 h were measured by semiquantitative Western blot analysis with anti-myc antibody. Sample Western blots for mNotch$^{\Delta E}$ and NICD are shown. β-Actin was used as loading control and detected with AC-74. *B*) Results of Western blot analysis shown in *A*. Data represent means ± SE of 4 experiments. $^{**}P < 0.01$ *vs.* vehicle-treated group.

N2a cells, which were stably overexpressing ectodomain truncated mouse Notch$^{\Delta E}$, with CA-074Me or typical γ-secretase inhibitors (compound E, DAPT, and L-685,458; **Fig. 4**). Western blot analysis indicated that treatment with compound E, DAPT, or L-685,458 significantly inhibited Notch processing, leading to a decrease in production of the Notch intracellular domain (NICD), as compared to treatment with vehicle. However, treatment with CA-074Me had no significant effect on the production of NICD. From these data, we conclude that cathepsin B, unlike APP, barely influences regulated intramembrane proteolysis of Notch or degradation of NICD.

Cathespin B is involved in the metabolism of CTFs independently of γ-secretase

Our results clearly suggest that cathepsin B and γ-secretase separately catalyze the proteolysis of CTFα and CTFβ, based on the following observations: chloroquine and NH_4Cl caused accumulation of CTFα in $PS1^{-/-}PS2^{-/-}$ cells; inhibition of cathepsin B caused accumulation of CTFs and AICD in APP_{NL}-H4 cells; and CA-074Me did not inhibit γ-secretase activity in the membrane fraction. To ascertain this conclusion, we investigated the effect of a combination of CA-074Me and γ-secretase inhibitor (compound E or L-685,458) in APP_{NL}-H4 cells (**Fig. 5*A*, *B***). Western blot analysis demonstrated that CTFs significantly accumulated following treatment with CA-074Me alone, γ-secretase inhibitor alone, or both of these compounds. Compound E is a peptidomimetic nontransition-state γ-secretase inhibitor, and L-685,458 is a hydroethylene dipeptide isostere-type transition-state analog. CA-074Me caused additional accumulation of CTFs in the presence of γ-secretase inhibitor; however, there was no difference in the level of extracellular Aβ, which is

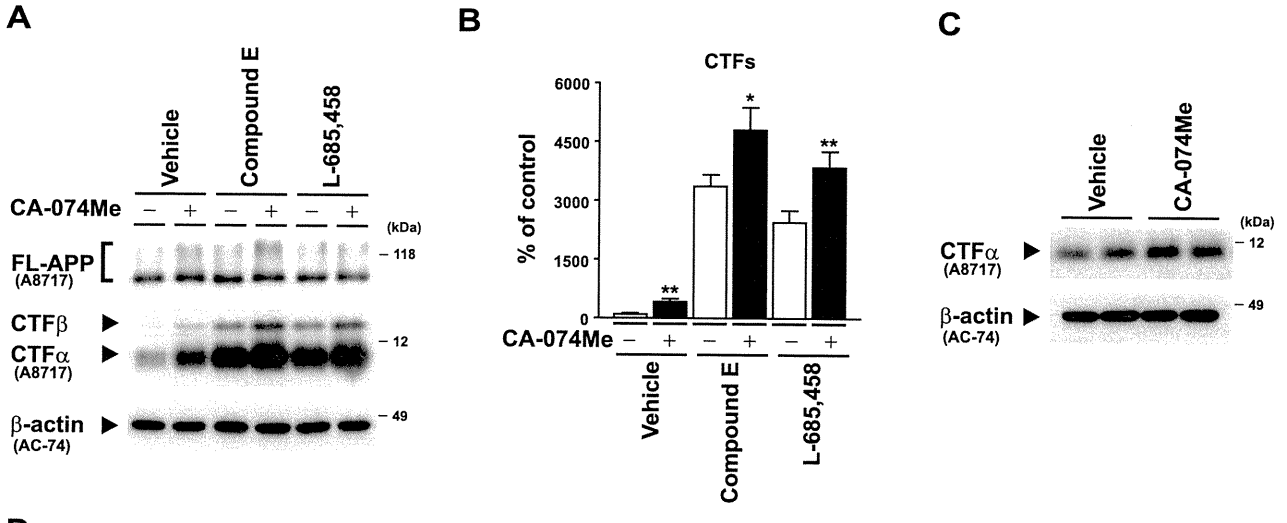

Figure 5. Cathespin B is involved in the metabolism of CTFs independently of γ-secretase. *A*) Amounts of CTFs (CTFα and CTFβ) in the cell lysates of APP_{NL}-H4 cells treated with a γ-secretase inhibitor (compound E or L-685,458; 1 μM) in combination with CA-074Me (10 μM) for 24 h were measured by semiquantitative Western blot analysis with A8717. *B*) Results of Western blot analysis shown in *A*. $^{*}P < 0.05$, $^{**}P < 0.01$ *vs.* CA-074Me-untreated group. *C*) Amounts of total CTFα in the cell lysate of $PS1^{-/-}PS2^{-/-}$ cells treated with CA-074Me (10 μM) for 24 h were measured by semiquantitative Western blot analysis with A8717. *D*) Results of Western blot analysis shown in *C*. $^{*}P < 0.05$ *vs.* vehicle-treated group. β-Actin was used as loading control and detected with AC-74 (*A*, *C*). Data represent means ± SE of 4 experiments.

produced by γ-secretase, in the presence or absence of CA-074Me (Supplemental Fig. S2).

In addition, we treated γ-secretase-deficient *PS1*$^{-/-}$ *PS2*$^{-/-}$ cells with CA-074Me. Western blot analysis with an anti-APP antibody showed that CTFα significantly accumulated in *PS1*$^{-/-}$*PS2*$^{-/-}$ cells following CA-074Me treatment (Fig. 5*C, D*). From these results, we concluded that cathepsin B had no effect on the production of CTFs from APP, and cathepsin B degrades CTFs independently of γ-secretase.

Cathepsin B degrades AICD *in vitro*

To examine whether AICD is directly degraded by cathepsin B, we subjected synthetic AICD to increasing quantities of purified cathepsin B for 60 min either in the absence or presence of CA-074 (**Fig. 6**). AICD degradation was assessed by Western blot using an anti-APP antibody. AICD was efficiently degraded by cathepsin B. This degradation by cathepsin B was promptly abolished by CA-074.

γ-Secretase prefers to degrade phosphorylated APP, whereas cathepsin B processes all APP substrates in the same way

Our above results indicate that cathepsin B contributes to the degradation of both CTFs and AICD independently of γ-secretase. We hypothesized that there was a regulatory factor for proteolysis of CTFs by cathepsin B or γ-secretase. A previous study demonstrated that CTFs phosphorylated at Thr668 facilitate their own processing by γ-secretase (22). We treated APP_{NL}-H4 cells with CA-074Me, β-secretase inhibitor IV, or L-685,458, and then assessed the levels of phosphorylated CTFs (pCTFs) and total CTFs containing phosphorylated and nonphosphorylated CTFs (npCTFs) (**Fig. 7*A, B***). We used CTFs containing CTFα and CTFβ, both of which are γ-secretase substrates. In the case of treatment with CA-074Me or β-secretase inhibitor IV, the ratios of the accumulated pCTFs to total CTFs did not show a significant difference. In contrast, the γ-secretase inhibitor L-685,458 caused an increase in this ratio. This significant increase in phosphorylated CTFs means that treatment with L-685,458, unlike treatment with CA-074Me, caused the increased accumulation of pCTFs over npCTFs.

To discern the difference between pCTFs and npCTFs for γ-secretase activity, we established a cell line that stably overexpressed APP mutated at a phosphorylation site (Thr to Ala on 668; APP_{NL_TA}-H4 cells) and then compared the accumulation rate of CTFs in APP_{NL}-H4 cells with that in APP_{NL_TA}-H4 cells (Fig. 7*C, D*). Although treatment with CA-074Me caused an increase in CTFs in both APP_{NL}-H4 cells and APP_{NL_TA}-H4 cells as compared to vehicle treatment in each cell, there was no significant difference in the accumulation rate of CTFs between APP_{NL}-H4 cells and APP_{NL_TA}-H4 cells. In contrast, treatment with L-685,458 caused accumulation of CTFs in both APP_{NL}-H4 cells and APP_{NL_TA}-H4 cells as compared to vehicle treatment in each cell, and the accumulation rate of CTFs in APP_{NL}-H4 cells was 4.5 times larger than that in APP_{NL_TA}-H4 cells. From these data, we could conclude that cathepsin B catalyzed the proteolysis of CTFs regardless of APP phosphorylation, whereas γ-secretase preferred pCTFs to npCTFs.

DISCUSSION

Cathepsin B, a well-characterized endosomal/lysosomal cysteine protease in mammalian cells, plays major roles in intracellular protein proteolysis (23, 24). Its specific inhibitor CA-074Me is a membrane-permeable analog of CA-074 that inhibits intracellular cathepsin B. CA-074Me is widely used *in vivo* and *in vitro*, although some

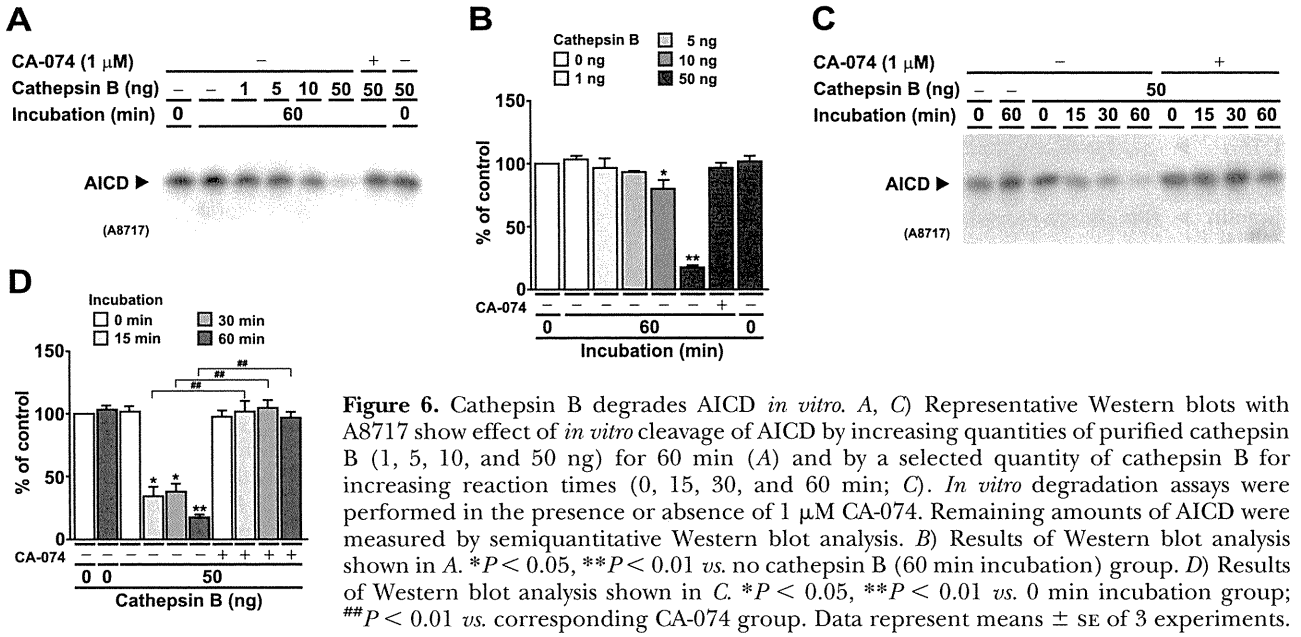

Figure 6. Cathepsin B degrades AICD *in vitro*. *A, C*) Representative Western blots with A8717 show effect of *in vitro* cleavage of AICD by increasing quantities of purified cathepsin B (1, 5, 10, and 50 ng) for 60 min (*A*) and by a selected quantity of cathepsin B for increasing reaction times (0, 15, 30, and 60 min; *C*). *In vitro* degradation assays were performed in the presence or absence of 1 μM CA-074. Remaining amounts of AICD were measured by semiquantitative Western blot analysis. *B*) Results of Western blot analysis shown in *A*. $*P < 0.05$, $**P < 0.01$ *vs.* no cathepsin B (60 min incubation) group. *D*) Results of Western blot analysis shown in *C*. $*P < 0.05$, $**P < 0.01$ *vs.* 0 min incubation group; $^{\#\#}P < 0.01$ *vs.* corresponding CA-074 group. Data represent means ± SE of 3 experiments.

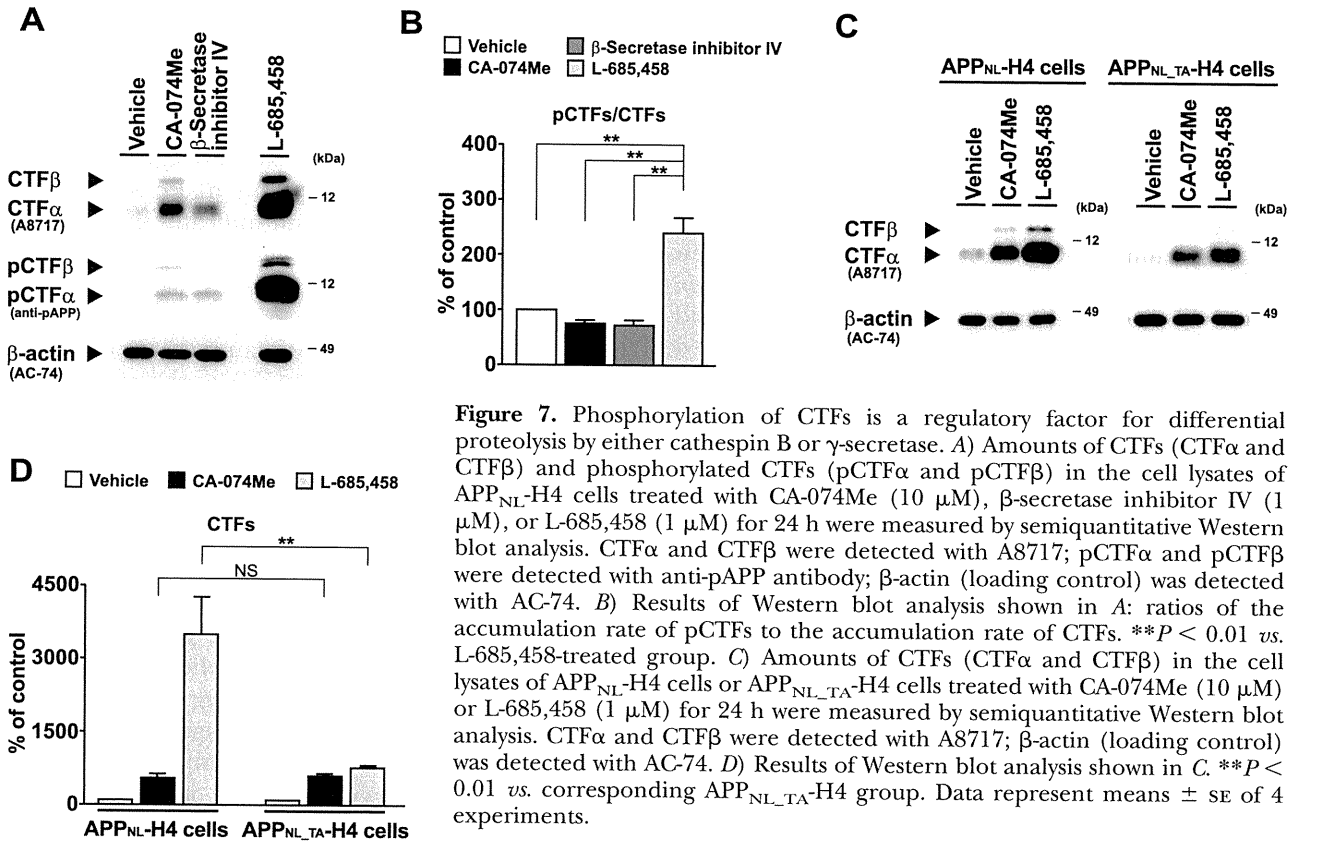

Figure 7. Phosphorylation of CTFs is a regulatory factor for differential proteolysis by either cathespin B or γ-secretase. *A*) Amounts of CTFs (CTFα and CTFβ) and phosphorylated CTFs (pCTFα and pCTFβ) in the cell lysates of APP_{NL}-H4 cells treated with CA-074Me (10 μM), β-secretase inhibitor IV (1 μM), or L-685,458 (1 μM) for 24 h were measured by semiquantitative Western blot analysis. CTFα and CTFβ were detected with A8717; pCTFα and pCTFβ were detected with anti-pAPP antibody; β-actin (loading control) was detected with AC-74. *B*) Results of Western blot analysis shown in *A*: ratios of the accumulation rate of pCTFs to the accumulation rate of CTFs. $^{**}P < 0.01$ *vs.* L-685,458-treated group. *C*) Amounts of CTFs (CTFα and CTFβ) in the cell lysates of APP_{NL}-H4 cells or APP_{NL_TA}-H4 cells treated with CA-074Me (10 μM) or L-685,458 (1 μM) for 24 h were measured by semiquantitative Western blot analysis. CTFα and CTFβ were detected with A8717; β-actin (loading control) was detected with AC-74. *D*) Results of Western blot analysis shown in *C*. $^{**}P < 0.01$ *vs.* corresponding APP_{NL_TA}-H4 group. Data represent means ± SE of 4 experiments.

studies suggest that CA-074Me deprives the specificity of cathepsin B by methyl esterification, to distinguish between inhibition of cathepsin B and that of other cysteine proteases, such as cathepsins H, L, and calpains (12–15). In the present study, we have demonstrated that cathepsin B possesses two novel roles in the metabolism of APP using a pharmacological approach with CA-074Me. Although chloroquine or NH_4Cl treatment has been reported to cause accumulation of both CTFs and AICD, which are a substrate and product of γ-secretase (11), CTFs have been recognized to be a substrate of only γ-secretase (1–4). As shown here, however, CTFs are also a substrate of cathepsin B; cathepsin B degraded CTFs with or without Swedish FAD mutation of APP independently of γ-secretase (Figs. 1, 2, and 5 and Supplemental Fig. S1) but did not affect Notch processing (Fig. 4). The key regulatory factor to determine an alternative pathway of CTF degradation in which cathepsin B or γ-secretase may be involved is phosphorylation at Thr668 of APP (Fig. 7). In addition, cathepsin B is also involved in degradation of AICD (Figs. 1, 2, and 6 and Supplemental Figs. S1 and S3).

The organelles in which cathepsin B degrades CTFs and AICD are a critical issue. In the hippocampal CA1 pyramidal neurons in mice, cathepsin B is primarily localized in the lysosomes and early endosomes (25). In the lysosome, one model posits that a KFERQ-like motif in APP, which is a specific pentapeptide lysosome-targeting consensus sequence (26), is recognized by a complex of chaperone proteins (including the heat shock 73-kDa protein, Hsc73) and then targeted to the lysosomal membrane for binding to LAMP2a, followed by transportation into the lysosomal lumen for degradation (27). Alternatively, Hsc73 binds to APP at another site unrelated to KFERQ sequence (28). However, in the early endosome, it is also possible that cathepsin B directly encounters CTFβ and AICD, which has been freshly produced, and degrades them. APP interacts with β-secretase [β-site APP-cleaving enzyme (BACE)] at the cell surface and then appears to be internalized together into early endosomes, undergoing β-cleavage (29), and PS also localizes in the early endosome, generating Aβ and AICD (30). On the other hand, because CTFα is thought to be produced by α-secretase at the cell surface (31), CTFα might be led to the lysosome by Hsc73, and thus be degraded by cathepsin B. Cathepsin B-mediated degradation of CTFα, CTFβ, and AICD might occur in different subcellular compartments and be regulated by different signaling.

The mode of regulation of cathepsin B activity remains unclear. Putative models include an endogenous cysteine protease inhibitor cystatin C (32) and a feedback mechanism based on AICD. AICD is assumed to function as a transcription activating factor for targeting *APP*, *BACE*, and *neprilysin* genes (33, 34). If gene expression of *APP* and *BACE* is up-regulated by AICD, Aβ levels should be increased. The major Aβ-degrading enzyme neprilysin, which is also likely to be upregulated, regulates levels of Aβ. Aβ42 activates cathepsin B (25), and then cathepsin B degrades CTFs and AICD to regulate transcription *via* AICD. An alternative name for cathepsin B is APP secretase (APPS), and it has been

suggested that cathepsin B is involved in proteolysis of FL-APP. Although it was initially demonstrated that cathepsin B has α-secretase-like activity through experiments with an artificial substrate that mimicked the α-secretase cleavage site (35), Hook *et al.* (14) showed that cathepsin B functioned as a β-secretase in the regulated secretory pathway against wild-type but not the Swedish mutation of APP. Moreover, it has been reported that cathepsin B has Aβ-degrading activity *in vivo* and *in vitro*, reducing the amount of amyloid plaques in aged AD model mice by lentivirus-mediated expression of cathepsin B (25). In the present study, cathepsin B seems to have no α- or β-secretase activity, and it may contribute to some Aβ degradation. However, cathepsin B is likely to be a multifunctional enzyme for APP metabolism; further studies are needed to establish its role in APP processing. First, for understanding the contribution of cathepsin B as β-secretase, it is important to estimate a ratio between Aβ present in the regulated secretory pathway and Aβ present in the constitutive secretory pathway in normal or AD brain. Second, from a different perspective, because treatment with CA-074Me results in acute inhibition of cathepsin B, there is no denying that a pharmacological approach with CA-074Me results in a different outcome than a genetic knockout experiment. As indicated above, cathepsin B-deficient mice exhibit no obvious phenotype, including the amounts of CTFs (25, 36); however, it has been suggested that cathepsin L compensates for the deficiency of cathepsin B. In this study, the treatment with E-64d, which is a broad cysteine protease inhibitor, caused accumulation of CTFα, CTFβ, and AICD. In cases in which CA-074Me loses the specificity of cathepsin B, cathepsin L also might be involved in degradation of CTFα, CTFβ, and AICD. Cathepsin B and L double-knockout mice are terminal during the second to fourth week of life and show neuronal loss (37). Although it has been reported that cathepsin B produces CTFβ in the regulated secretory pathway (14, 38, 39), our study clearly showed that cathepsin B degrades both CTFs and AICD. Since CTFs themselves are toxic (40) and AICD transgenic mice display age-dependent neurodegeneration (41), it may not be advisable to inhibit cathepsin B activity to treat AD, which may worsen rather than improve AD.

Protein phosphorylation, in particular, plays a significant role in a wide range of molecular and cellular biology. Reversible phosphorylation of proteins is an important regulatory mechanism that may influence conformational changes in the structure, altered localization, and enzymatic activity regulation. Phosphorylation of APP has been previously reported to induce a conformational change in the cytoplasmic region to alter interaction with Fe65, a neuronal-specific adaptor protein (42). The transfection of APP containing a Thr to Glu mutation (mimics phosphorylation) with Fe65 increases Aβ levels (42). Phosphorylation by stress-induced c-Jun N-terminal kinase (JNK) enhances proteolysis of pCTFs by γ-secretase (22). Although further investigation of the relationship between phosphorylation of APP and cathepsin B is required, we have provided indirect evidence that cathepsin B degrades CTFs at a constant rate without distinction for the phosphorylation state of the CTF (Fig. 7). Interestingly, inhibition of cathepsin B showed no significant difference in Aβ levels in our experimental paradigm (Supplemental Fig. S2). This result indicates that cathepsin B and γ-secretase share CTFs as a substrate but do not compete against each other. However, γ-secretase preferably hydrolyzed pCTFs over npCTFs (Fig. 7). Why inhibition of γ-secretase causes an increase in the ratio of the accumulation rate of pCTFs to the accumulation rate of CTFs and why inhibition of cathepsin B does not show this result are interesting puzzles still to be resolved. The significant decrease in the accumulation rate of CTFs in APP_{NL_TA}-H4 cells, as compared to that in APP_{NL}-H4 cells, when the γ-secretase inhibitor L-685,458 was administered confirms that APP phosphorylation regulates proteolysis of CTFs by γ-secretase. Cyclin-dependent kinase-5 (Cdk5), glycogen synthase kinase-3β (GSK-3β), and JNK are believed to phosphorylate APP at Thr668 (43), suggesting that inhibitors of these kinases would be effective drugs in the treatment of AD. Indeed, the GSK-3 inhibitor lithium chloride reduces Aβ levels (44). Kinase inhibitors, unlike γ-secretase inhibitors, would be expected to specifically block γ-cleavage of CTFs derived from APP without inhibition of γ-cleavage of other substrates (44). Furthermore, because these kinases also phosphorylate tau, which is a major component of neurofibrillary tangles, inhibition of these kinases decreases levels of hyperphosphorylated tau, preventing neurodegeneration and neuronal loss without Aβ reduction (45). In addition, based on our results and previous findings, serine/threonine phosphatases are also drug candidates. Protein phosphatase 2A (PP2A) is one of the most important phosphatases in the brain (46). PP2A activity decreases in AD brains (47), suggesting that Aβ is overproduced by activation of γ-secretase. This decreased PP2A activity also promotes phosphorylation of tau (47).

We propose the following model for roles of cathepsin B in APP processing. APP is metabolized by α- and β-secretase to generate CTFα and CTFβ, respectively. γ-Secretase and cathepsin B continuously hydrolyze CTFs; however, γ-secretase prefers the phosphorylated form of CTFs as substrates and then produces AICD from CTFs. pCTFs, npCTFs, and AICD are substrates for cathepsin B.

In summary, the present data demonstrate that cathepsin B contributes to the degradation of CTFs and AICD independently of α-, β-, and γ-secretases and that γ-secretase prefers pCTFs to npCTFs but cathepsin B does not. This study also suggests that reducing this phosphorylation may be a candidate for therapeutic intervention in AD. FJ

The authors thank Dr. Raphael Kopan (Washington University, St. Louis, MO, USA) for providing a plasmid (ΔEMV:

pCS2/Notch$^{\Delta E}$), Dr. Bart De Strooper (Katholieke Universiteit Leuven, Leuven, Belgium) for providing PS1 and PS2 double-knockout MEF *PS1*$^{-/-}$*PS2*$^{-/-}$ cells, and Drs. Taisuke Tomita and Takeshi Iwatsubo (The University of Tokyo, Tokyo, Japan) for providing mNotch$^{\Delta E}$-N2a cells. The authors also thank Dr. Kazumi Ishidoh (Tokushima Bunri University, Tokushima, Japan) for his valuable advice. This work was supported by the Regional Innovation Cluster Program (City Area Type; Central Saitama Area), the Shimabara Science Promotion Foundation, and a Grant-in-Aid for Scientific Research (C; 20590260) from the Japan Society for the Promotion of Science.

REFERENCES

1. Zheng, H., and Koo, E. H. (2006) The amyloid precursor protein: beyond amyloid. *Mol. Neurodegener.* **1,** 5
2. Marks, N., and Berg, M. J. (2008) Neurosecretases provide strategies to treat sporadic and familial Alzheimer disorders. *Neurochem. Int.* **52,** 184–215
3. Jacobsen, K. T., and Iverfeldt, K. (2009) Amyloid precursor protein and its homologues: a family of proteolysis-dependent receptors. *Cell. Mol. Life Sci.* **66,** 2299–2318
4. Panza, F., Solfrizzi, V., Frisardi, V., Capurso, C., D'Introno, A., Colacicco, A. M., Vendemiale, G., Capurso, A., and Imbimbo, B. P. (2009) Disease-modifying approach to the treatment of Alzheimer's disease: from α-secretase activators to γ-secretase inhibitors and modulators. *Drugs Aging* **26,** 537–555
5. Tomita, T. (2009) Secretase inhibitors and modulators for Alzheimer's disease treatment. *Expert Rev. Neurother.* **9,** 661–679
6. Doerfler, P., Shearman, M. S., and Perlmutter, R. M. (2001) Presenilin-dependent γ-secretase activity modulates thymocyte development. *Proc. Natl. Acad. Sci. U. S. A.* **98,** 9312–9317
7. Dovey, H. F., John, V., Anderson, J. P., Chen, L. Z., de Saint Andrieu, P., Fang, L. Y., Freedman, S. B., Folmer, B., Goldbach, E., Holsztynska, E. J., Hu, K. L., Johnson-Wood, K. L., Kennedy, S. L., Kholodenko, D., Knops, J. E., Latimer, L. H., Lee, M., Liao, Z., Lieberburg, I. M., Motter, R. N., Mutter, L. C., Nietz, J., Quinn, K. P., Sacchi, K. L., Seubert, P. A., Shopp, G. M., Thorsett, E. D., Tung, J. S., Wu, J., Yang, S., Yin, C. T., Schenk, D. B., May, P. C., Altstiel, L. D., Bender, M. H., Boggs, L. N., Britton, T. C., Clemens, J. C., Czilli, D. L., Dieckman-McGinty, D. K., Droste, J. J., Fuson, K. S., Gitter, B. D., Hyslop, P. A., Johnstone, E. M., Li, W.-Y., Little, S. P., Mabry, T. E., Miller, F. D., Ni, B., Nissen, J. S., Porter, W. J., Potts, B. D., Reel, J. K., Stephenson, D., Su, Y., Shipley, L. A., Whitesitt, C. A., Yin T., and Audia, J. E. (2001) Functional gamma-secretase inhibitors reduce beta-amyloid peptide levels in brain. *J. Neurochem.* **76,** 173–181
8. Gu, Y., Misonou, H., Sato, T., Dohmae, N., Takio, K., and Ihara, Y. (2001) Distinct intramembrane cleavage of the β-amyloid precursor protein family resembling γ-secretase-like cleavage of Notch. *J. Biol. Chem.* **276,** 35235–35238
9. Milano, J., McKay, J., Dagenais, C., Foster-Brown, L., Pognan, F., Gadient, R., Jacobs, R. T., Zacco, A., Greenberg, B., and Ciaccio, P. J. (2004) Modulation of notch processing by γ-secretase inhibitors causes intestinal goblet cell metaplasia and induction of genes known to specify gut secretory lineage differentiation. *Toxicol. Sci.* **82,** 341–358
10. Eisele, Y. S., Baumann, M., Klebl, B., Nordhammer, C., Jucker, M., and Kilger, E. (2007) Gleevec increases levels of the amyloid precursor protein intracellular domain and of the amyloid-β-degrading enzyme neprilysin. *Mol. Biol. Cell* **18,** 3591–3600
11. Vingtdeux, V., Hamdane, M., Bégard, S., Loyens, A., Delacourte, A., Beauvillain, J. C., Buée, L., Marambaud, P., and Sergeant, N. (2007) Intracellular pH regulates amyloid precursor protein intracellular domain accumulation. *Neurobiol. Dis.* **25,** 686–696
12. Hook, V. Y., Kindy, M., and Hook, G. (2008) Inhibitors of cathepsin B improve memory and reduce β-amyloid in transgenic Alzheimer disease mice expressing the wild-type, but not the Swedish mutant, β-secretase site of the amyloid precursor protein. *J. Biol. Chem.* **283,** 7745–7753
13. Van Acker, G. J., Saluja, A. K., Bhagat, L., Singh, V. P., Song, A. M., and Steer, M. L. (2002) Cathepsin B inhibition prevents trypsinogen activation and reduces pancreatitis severity. *Am. J. Physiol. Gastrointest. Liver Physiol.* **283,** G794–G800
14. Hook, V., Toneff, T., Bogyo, M., Greenbaum, D., Medzihradszky, K. F., Neveu, J., Lane, W., Hook, G., and Reisine, T. (2005) Inhibition of cathepsin B reduces β-amyloid production in regulated secretory vesicles of neuronal chromaffin cells: evidence for cathepsin B as a candidate β-secretase of Alzheimer's disease. *Biol. Chem.* **386,** 931–940
15. Ha, S. D., Martins, A., Khazaie, K., Han, J., Chan, B. M., and Kim, S. O. (2008) Cathepsin B is involved in the trafficking of TNF-α-containing vesicles to the plasma membrane in macrophages. *J. Immunol.* **181,** 690–697
16. Asai, M., Iwata, N., Tomita, T., Iwatsubo, T., Ishiura, S., Saido, T. C., and Maruyama, K. (2010) Efficient four-drug cocktail therapy targeting amyloid-β peptide for Alzheimer's disease. *J. Neurosci. Res.* **88,** 3588–3597
17. Asai, M., Iwata, N., Yoshikawa, A., Aizaki, Y., Ishiura, S., Saido, T. C., and Maruyama, K. (2007) Berberine alters the processing of Alzheimer's amyloid precursor protein to decrease Aβ secretion. *Biochem. Biophys. Res. Commun.* **352,** 498–502
18. Herreman, A., Serneels, L., Annaert, W., Collen, D., Schoonjans, L., and De Strooper, B. (2000) Total inactivation of γ-secretase activity in presenilin-deficient embryonic stem cells. *Nat. Cell Biol.* **2,** 461–462
19. De Duve, C., de Barsy, T., Poole, B., Trouet, A., Tulkens, P., and Van Hoof, F. (1974) Commentary. Lysosomotropic agents. *Biochem. Pharmacol.* **23,** 2495–2531
20. Gekle, M., Mildenberger, S., Freudinger, R., and Silbernagl, S. (1995) Endosomal alkalinization reduces J_{max} and K_m of albumin receptor-mediated endocytosis in OK cells. *Am. J. Physiol.* **268,** F899–F906
21. Yagishita, S., Morishima-Kawashima, M., Ishiura, S., and Ihara, Y. (2008) Aβ46 is processed to Aβ40 and Aβ43, but not to Aβ42, in the low density membrane domains. *J. Biol. Chem.* **283,** 733–738
22. Vingtdeux, V., Hamdane, M., Gompel, M., Bégard, S., Drobecq, H., Ghestem, A., Grosjean, M. E., Kostanjevecki, V., Grognet, P., Vanmechelen, E., Buée, L., Delacourte, A., and Sergeant, N. (2005) Phosphorylation of amyloid precursor carboxy-terminal fragments enhances their processing by a gamma-secretase-dependent mechanism. *Neurobiol. Dis.* **20,** 625–637
23. Nakanishi, H. (2003) Neuronal and microglial cathepsins in aging and age-related diseases. *Ageing Res. Rev.* **2,** 367–381
24. Guha, S., and Padh, H. (2008) Cathepsins: fundamental effectors of endolysosomal proteolysis. *Indian J. Biochem. Biophys.* **45,** 75–90
25. Mueller-Steiner, S., Zhou, Y., Arai, H., Roberson, E. D., Sun, B., Chen, J., Wang, X., Yu, G., Esposito, L., Mucke, L., and Gan, L. (2006) Antiamyloidogenic and neuroprotective functions of cathepsin B: implications for Alzheimer's disease. *Neuron* **51,** 703–714
26. Dice, J. F., and Terlecky, S. R. (1990) Targeting of cytosolic proteins to lysosomes for degradation. *Crit. Rev. Ther. Drug Carrier Syst.* **7,** 211–233
27. Cuervo, A. M. (2004) Autophagy: many paths to the same end. *Mol. Cell. Biochem.* **263,** 55–72
28. Kouchi, Z., Sorimachi, H., Suzuki, K., and Ishiura, S. (1999) Proteasome inhibitors induce the association of Alzheimer's amyloid precursor protein with Hsc73. *Biochem. Biophys. Res. Commun.* **254,** 804–810
29. Kinoshita, A., Fukumoto, H., Shah, T., Whelan, C. M., Irizarry, M. C., and Hyman, B. T. (2003) Demonstration by FRET of BACE interaction with the amyloid precursor protein at the cell surface and in early endosomes. *J. Cell Sci.* **116,** 3339–3346
30. Vetrivel, K. S., Cheng, H., Lin, W., Sakurai, T., Li, T., Nukina, N., Wong, P. C., Xu, H., and Thinakaran, G. (2004) Association of γ-secretase with lipid rafts in post-Golgi and endosome membranes. *J. Biol. Chem.* **279,** 44945–44954
31. Thinakaran, G., and Koo, E. H. (2008) Amyloid precursor protein trafficking, processing, and function. *J. Biol. Chem.* **283,** 29615–29619
32. Sun, B., Zhou, Y., Halabisky, B., Lo, I., Cho, S. H., Mueller-Steiner, S., Devidze, N., Wang, X., Grubb, A., and Gan, L. (2008)

Cystatin C-cathepsin B axis regulates amyloid beta levels and associated neuronal deficits in an animal model of Alzheimer's disease. *Neuron* **60,** 247–257
33. Von Rotz, R. C., Kohli, B. M., Bosset, J., Meier, M., Suzuki, T., Nitsch, R. M., and Konietzko, U. (2004) The APP intracellular domain forms nuclear multiprotein complexes and regulates the transcription of its own precursor. *J. Cell Sci.* **117,** 4435–4448
34. Pardossi-Piquard, R., Petit, A., Kawarai, T., Sunyach, C., Alves da Costa, C., Vincent, B., Ring, S., D'Adamio, L., Shen, J., Müller, U., St. George Hyslop, P., and Checler, F. (2005) Presenilin-dependent transcriptional control of the Aβ-degrading enzyme neprilysin by intracellular domains of βAPP and APLP. *Neuron* **46,** 541–554
35. Tagawa, K., Kunishita, T., Maruyama, K., Yoshikawa, K., Kominami, E., Tsuchiya, T., Suzuki, K., Tabira, T., Sugita, H., and Ishiura, S. (1991) Alzheimer's disease amyloid β-clipping enzyme (APP secretase): identification, purification, and characterization of the enzyme. *Biochem. Biophys. Res. Commun.* **177,** 377–387
36. Deussing, J., Roth, W., Saftig, P., Peters, C., Ploegh, H. L., and Villadangos, J. A. (1998) Cathepsins B and D are dispensable for major histocompatibility complex class II-mediated antigen presentation. *Proc. Natl. Acad. Sci. U. S. A.* **95,** 4516–4521
37. Felbor, U., Kessle, B., Mothes, W., Goebel, H. H., Ploegh, H. L., Bronson, R. T., and Olsen, B. R. (2002) Neuronal loss and brain atrophy in mice lacking cathepsins B and L. *Proc. Natl. Acad. Sci. U. S. A.* **99,** 7883–7888
38. Hook, V. Y., Kindy, M., Reinheckel, T., Peters, C., and Hook, G. (2009) Genetic cathepsin B deficiency reduces β-amyloid in transgenic mice expressing human wild-type amyloid precursor protein. *Biochem. Biophys. Res. Commun.* **386,** 284–288
39. Klein, D. M., Felsenstein, K. M., and Brenneman, D. E. (2009) Cathepsins B and L differentially regulate amyloid precursor protein processing. *J. Pharmacol. Exp. Ther.* **328,** 813–821
40. Kim, S. H., and Suh, Y. H. (1996) Neurotoxicity of a carboxyl-terminal fragment of the Alzheimer's amyloid precursor protein. *J. Neurochem.* **67,** 1172–1182
41. Ghosal, K., Vogt, D. L., Liang, M., Shen, Y., Lamb, B. T., and Pimplikar, S. W. (2009) Alzheimer's disease-like pathological features in transgenic mice expressing the APP intracellular domain. *Proc. Natl. Acad. Sci. U. S. A.* **106,** 18367–18372
42. Ando, K., Iijima, K. I., Elliott, J. I., Kirino, Y., and Suzuki, T. (2001) Phosphorylation-dependent regulation of the interaction of amyloid precursor protein with Fe65 affects the production of β-amyloid. *J. Biol. Chem.* **276,** 40353–40361
43. Suzuki, T., and Nakaya, T. (2008) Regulation of amyloid β-protein precursor by phosphorylation and protein interactions. *J. Biol. Chem.* **283,** 29633–29637
44. Rockenstein, E., Torrance, M., Adame, A., Mante, M., Bar-on, P., Rose, J. B., Crews, L., and Masliah, E. (2007) Neuroprotective effects of regulators of the glycogen synthase kinase-3β signaling pathway in a transgenic model of Alzheimer's disease are associated with reduced amyloid precursor protein phosphorylation. *J. Neurosci.* **27,** 1981–1991
45. Citron, M. (2010) Alzheimer's disease: strategies for disease modification. *Nat. Rev. Drug Discov.* **9,** 387–398
46. Janssens, V., and Goris, J. (2001) Protein phosphatase 2A: a highly regulated family of serine/threonine phosphatases implicated in cell growth and signaling. *Biochem. J.* **353,** 417–439
47. Liu, F., Grundke-Iqbal, I., Iqbal, K., and Gong, C. X. (2005) Contributions of protein phosphatases PP1, PP2A, PP2B and PP5 to the regulation of tau phosphorylation. *Eur. J. Neurosci.* **22,** 1942–1950

Received for publication February 1, 2011.
Accepted for publication June 23, 2011.

Neuroscience Letters 503 (2011) 234–239

Contents lists available at SciVerse ScienceDirect

Neuroscience Letters

journal homepage: www.elsevier.com/locate/neulet

Protective role of the ubiquitin binding protein Tollip against the toxicity of polyglutamine-expansion proteins

Asami Oguro[a,1], Hiroshi Kubota[b], Miho Shimizu[c], Shoichi Ishiura[a], Yoriko Atomi[d,*]

[a] Department of Life Sciences, The Graduate School of Arts and Sciences, The University of Tokyo, Meguro-ku, Tokyo 153-8902, Japan
[b] Department of Life Science, Faculty and Graduate School of Engineering and Resource Science, Akita University, 1-1 Tegatagakuen-cho, Akita 010-8502, Japan
[c] Graduate School of Information Science and Technology, The University of Tokyo, 7-3-1, Hongo, Bunkyo-ku, Tokyo 113-8656, Japan
[d] The University of Tokyo, Radioisotope Center Cell to Body Dynamics Laboratory 1 2-11-16, Yayoi, Bunkyo-ku, Tokyo 113-0032, Japan

ARTICLE INFO

Article history:
Received 7 January 2011
Received in revised form 3 August 2011
Accepted 22 August 2011

Keywords:
Aggregation
Huntingtin
Polyglutamine
Tollip

ABSTRACT

Huntington disease (HD) is caused by the expansion of polyglutamine (polyQ) repeats in the amino-terminal of hungtintin (htt). PolyQ-expanded htt forms intracellular ubiquitinated aggregates in neurons and causes neuronal cell death. Here, utilizing a HD cellular model, we report that Tollip, an ubiquitin binding protein that participates in intracellular transport *via* endosomes, co-localizes with and stimulates aggregation of polyQ-expanded amino-terminal htt. Furthermore, we demonstrate that Tollip protects cells against the toxicity of polyQ-expanded htt. We propose that association of Tollip with polyubiquitin accelerates aggregation of toxic htt species into inclusions and thus provides a cell protective role by sequestration.

Huntington disease (HD, OMIM-143100) is a progressive autosomal dominant neurodegenerative disorder caused by expansion of polyglutamine (polyQ) in the hungtintin (htt) protein. The gene encoding htt contains a CAG repeat in exon 1, and this repeat is expanded in HD patients. Although full-length htt is ubiquitously expressed as a 348-kDa cytoplasmic protein, the amino-terminal fragments of polyQ expanded htt (htt^{pQ}) tend to form ubiquitinated intracellular aggregates and exert toxicity in neuronal cells [1]. Htt^{pQ} has been shown to cause protein misfolding, aberrant transcription, chaperone activity inhibition and proteasome dysfunction, although the exact molecular mechanism by which polyQ exerts cellular toxicity is unknown [8].

Tollip (Toll-interacting protein) is a ubiquitin binding protein that is involved in sorting of ubiquitinated proteins from endosomes to lysosomes for degradation including that of interleukin-1 receptor (IL-1R) [3,4]. Tollip binds to ubiquitin through the CUE (coupling of ubiquitin to ER degradation) domain and interacts with clathrin and Tom1 (target of Myb protein 1), leading to formation of a multi protein complex for protein degradation [9]. Tollip is localized in endosomes, and disruption of the *Tollip* gene results in accumulation of IL-1R in endosomes and deficiency in lysosomal degradation of IL-1R [3]. Tollip is reported as a protein concentrated in polyglutamine aggregates [5], and the ubiquitin binding protein p62 (also known as sequestosome 1) is known to mediate autophagy-dependent clearance of polyQ aggregates with accelerating htt^{pQ} aggregation [13]. These observations suggested that, like p62, Tollip may be involved in htt^{pQ} aggregation and degradation through ubiquitin binding and membrane sorting activities. Thus, we decided to analyze the role of Tollip in htt^{pQ} aggregation, trafficking and cytotoxicity in neuronal cells.

Experimental procedures: The *htt* expression constructs, pIND-tNhtt-EGFP-60Q and pIND-tNhtt-EGFP-150Q, and the generation of the stable Neuro2a cell lines expressing htt proteins were provided by Dr. Nukina [7]. The stable cell lines (HD60Q and HD150Q) were maintained in DMEM supplemented with 10% fetal bovine serum, 0.4 mg/ml Zeocin and 0.4 mg/ml G418 (Sigma). All transfections were performed using the Lipofectamine 2000 reagent (Invitrogen) according to the manufacturer's instructions. To knockdown *Tollip*, cells were transiently transfected with *Tollip* stealth siRNA duplex oligoribonucleotides, 5′-UCUCAAGGUAGAACGAGUCCACACC-3′ and 5′-GGUGUGGACUCGUUCUACCUUGAGA-3′ or Stealth RNAi Negative Control Duplexes, while *Tollip* overexpression was achieved by transiently transfected with the RFP-Tollip expression vector [mouse *Tollip* cloned into the RFPc1 vector (Invitrogen)]. To assess if levels of *Tollip* affected aggregate formation, cells were transiently cotransfected with either GFP-Tollip (or empty GFP cassette) and *htt* (20Q, 80Q or 87Q) exon1 fused with a V5 tag. Twelve hours after transfection, 1 μM of ponasterone A (Invitrogen) for induction of

* Corresponding author. Tel.: +81 3 5841 3055; fax: +81 3 5841 3055.
E-mail addresses: oguroasami@ucla.edu (A. Oguro), hkubota@ipc.akita-u.ac.jp (H. Kubota), mshimizu@ynl.t.u-tokyo.ac.jp (M. Shimizu), cishiura@mail.ecc.u-tokyo.ac.jp (S. Ishiura), atomi@bio.c.u-tokyo.ac.jp (Y. Atomi).
[1] Present address: Department of Neurology, David Geffen School of Medicine, University of California, Los Angeles, CA 90095, USA.

0304-3940/$ – see front matter © 2011 Elsevier Ireland Ltd. All rights reserved.
doi:10.1016/j.neulet.2011.08.043

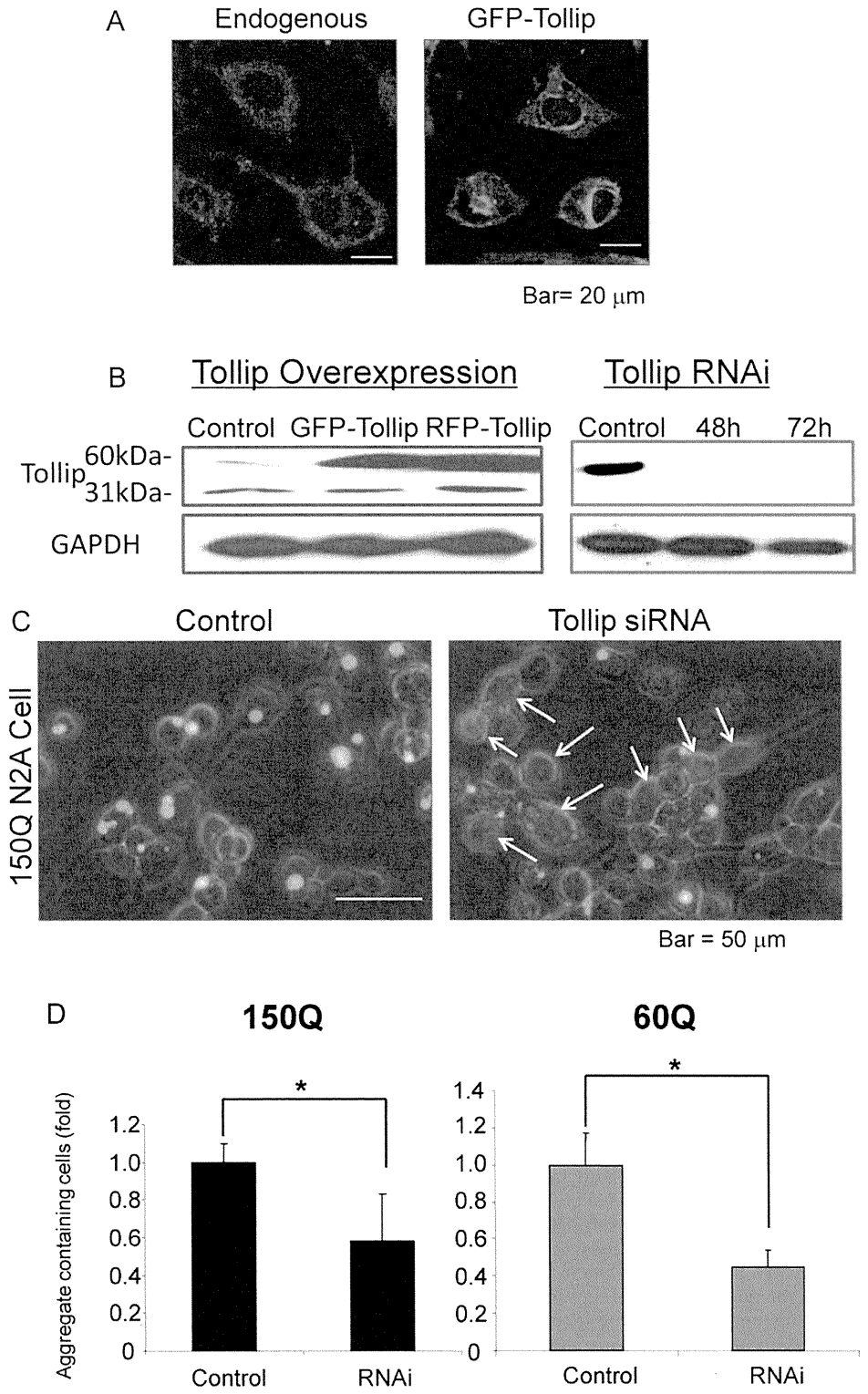

Fig. 1. Tollip associates with aggregates of polyQ-expanded htt and affects polyQ aggregation. (A) GFP-Tollip overexpression shows the same localization pattern as endogenous Tollip in the htt150Q Neuro2a cell line without induction. At 48 h of transfection, cells were analyzed by immunostaining. Tollip distributed in small granular particles in the cytoplasm. Bar = 20 μm. (B) Cells were transiently transfected with GFP-*Tollip* or RFP-*Tollip* for 48 h (left), or *Tollip* siRNA for 48–72 h (right). Tollip expression level was analyzed by Western blotting. (C) Htt150Q-expressing cells were transfected with *Tollip* siRNA or control siRNA for 48 h. *Tollip* siRNA treated cells exhibits decreased htt^{pQ} aggregation. Arrows indicate GFP-positive cells that do not form htt^{pQ} aggregates. Bar = 50 μm. (D) *Tollip* knockdown inhibits htt^{pQ} aggregation. HD150Q and HD60Q cells were transfected with *Tollip* siRNA or control siRNA, and aggregate-containing cells were counted ($n = 3$). *, $p < 0.01$.

aggregation was added to the culture and then incubated for an additional 24 h. To count aggregate containing cells, 1×10^3 cells were seeded into chambered slides, and aggregate containing cells were manually counted using a fluorescence microscope. To test cell death, 5×10^5 cells were inoculated into each well of 6-well plates, 48 h following transfection, cells were differentiated with 5 mM dibutyryl cyclic AMP in the presence of 1 μM of ponasterone A and allowed to incubate for three days. Aggregate counting experiments were performed after cells were transiently transfected with *Tollip* stealth siRNA duplex or plasmid expression vector (transfection efficiency was almost 90% in Neuro2a cells), and more than 200 cells were counted. Dead cells were counted by propidium iodide staining as described previously [10], and cell viability was measured using Titer Blue assay kit (Promega). Statistical analysis was performed by Student's *t*-test. To inhibit the proteasome, cells were treated with carbobenzoxy-L-leucyl-L-leucyl-L-leucinal (MG-132; Wako, Osaka, Japan) and microtubule destabilization was performed using nocodazole (Sigma).

For immunofluorescence experiments, cells were fixed with 4% paraformaldehyde in PBS for 20 min and blocked with 0.2% BSA in TBST (Tris-Buffered Saline Tween-20) for 1 h. Fixed cells were incubated with antibodies against Tollip (rabbit polyclonal, Ref. [21]), vimentin (mouse monoclonal, Abcam), EEA1 (mouse monoclonal, BD Transduction) or syntaxin-7 (rabbit polyclonal, Abcam) at 1:50 dilution (4 °C, overnight). After several washes with TBST, cells were incubated with Alexa488- or Alexa546-conjigated secondary antibodies (1:2000) for 1 h. After washes, cells were mounted in antifade solution. Immunofluoresent staining of Tollip in HD150Q cells was carried out as described [7]. Solubility of proteins was examined as follows: cells were scraped, homogenized and lysed in PBS supplemented with protease inhibitor cocktail (Sigma) on ice. Cell lysates were briefly sonicated, centrifuged for 10 min at 15,000 × *g* at 4 °C, and supernatants (soluble fraction) and pellet (insoluble fraction) were analyzed by Western blotting [21].

To examine whether Tollip affects htt^{pQ} aggregation, we established Tollip overexpression and knockdown system *in vitro* (Fig. 1A and B). After overexpression of Tollip using GFP-Tollip construct, transfected Neuro2a cells showed essentially the same localization pattern as endogenous Tollip in cytosol (Fig. 1A), while expression levels of GFP/RFP-Tollip were significantly higher than endogenous Tollip (Fig. 1B, left). Treatment of Neuro2a cells with *Tollip* siRNA diminished endogenous Tollip protein after 48 h through 72 h (Fig. 1B, right). Under the Tollip knockdown conditions, the number of cells that contain htt (150Q and 60Q) aggregates was significantly reduced to approximately 50% (Fig. 1C and D). These results indicate that Tollip stimulates polyQ aggregation in living cells.

Since many polyQ binding proteins affects polyQ-dependent cell death [18], we hypothesized that association of Tollip with htt^{pQ} aggregates may affect polyQ toxicity. Overexpression of Tollip significantly stimulated aggregation of GFP-htt60Q (Fig. 2A), and suppressed cell death in the htt80Q and htt87Q lines (Fig. 2B). In contrast, Tollip overexpression provided no significant difference on the cell death of htt20Q expressing cells (Fig. 2B). Thus, Tollip protects cells against the toxicity of expanded polyQ concomitant with stimulating htt^{pQ} aggregation into aggresomes.

Previous reports indicated that Tollip contains the ubiquitin binding CUE domain [15,20]. Ubiquitin binding motifs are also found in p62 and ubiquilin1, and these proteins function in the ubiquitin–proteasome pathway [6,18]. To investigate whether Tollip distribution is affected by proteasomal inhibition, Neuro2a cells treated with the proteasome inhibitor MG-132 and localization of Tollip was analyzed by immunofluorescence microscopy (Fig. 3A). MG-132 treatment frequently induced formation of juxtanuclear Tollip-containing inclusions surrounded by vimentin, of which specific structure is a marker of the aggresome. We next treated cells

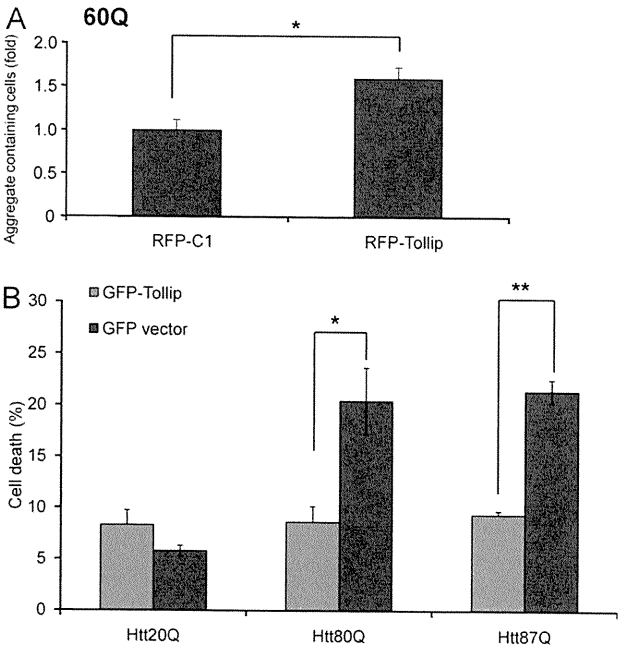

Fig. 2. Overexpression of Tollip induces htt^{pQ} aggregation and reduces cell death. (A) Htt-expressing cells were transfected with RFP-Tollip or RFP-C as a control, and aggregate-containing cells were counted ($n = 4$). (B) Tollip protects cells against the toxicity of htt^{pQ}. Neuro2a cells were transiently co-transfected with htt (20Q, 80Q or 87Q) and GFP-Tollip (or GFP as a control). Cells were differentiated in the presence of 5 mM dbcAMP. Cell death was analyzed by propidium iodide staining ($n = 4$). More than 300 cells were counted for each experiment. *, $p < 0.01$; **, $p < 0.001$.

with the microtubule-destabilizing drug nocodazole, because formation and maintenance of aggresomes are known to be dependent on microtubule-dependent transport system. Treatment of cells with nocodazole resulted in a more dispersed distribution of Tollip in the cytoplasm in the presence of MG-132. These results indicate that Tollip is concentrated in the aggresome and/or in the region surrounding the aggresome. Centrifugal fractionation indicated that Tollip was present in the insoluble fractions after MG132 treatment (Fig. 3B). Given the insoluble nature of the aggresome, this suggests that Tollip is associated with this structure.

Tollip is known to play a role in endosomal protein trafficking; therefore we performed immunostaining of Tollip with EEA1 (an early endosome marker) or syntaxin-7 (a late endosome marker) in cultured Neuro2a and HEK293 cells after treatment with MG-132 (Fig. 4A). Tollip was rarely found in early endosomes but partly distributed in late endosomes under normal conditions. After MG132 treatment, however, Tollip was highly colocalized with the late endosome marker syntaxin-7. Previous studies indicated that Tollip is known to be accumulated in htt^{pQ} inclusions in the brain of HD model mouse (R6/1) [21]. We thus tested whether Tollip associates with htt^{pQ} aggregates in the HD cellular model [7]. Expression of GFP-htt150Q was induced for 24 h in the presence of ponasterone A, and localization of Tollip was analyzed by immunofluorescence staining. Strong Tollip staining surrounding htt^{pQ} aggregates was observed (Fig. 4B, upper). We also analyzed localization of syntaxin-7 in htt150Q expressing cells and found that syntaxin-7 colocalizes with htt^{pQ} aggregates (Fig. 4B, lower). Thus, Tollip function may be associated with recruitment of misfolded proteins to aggresomes *via* late endosomes, including the case of htt^{pQ}. Under MG132-induced stress conditions, overexpression of Tollip significantly protected cells from the toxicity of the proteasome inhibitor (Fig. 4C, left). Furthermore, knockdown of Tollip significantly decreased cell viability of MG132-treated cells (Fig. 4C, right). These results indicate that

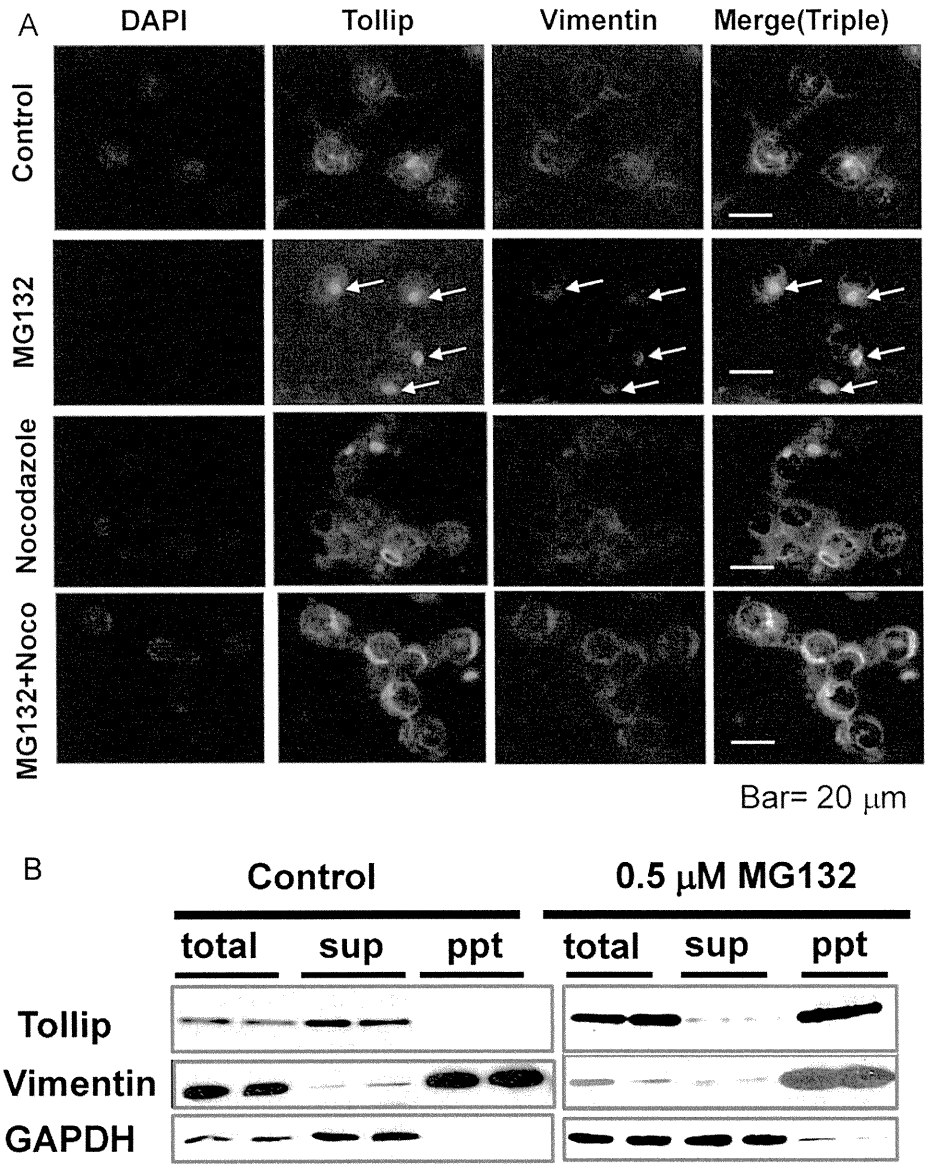

Fig. 3. Proteasome inhibition causes accumulation of Tollip in the aggresome. (A) After treatment with 0.5 μM MG-132 for 24 h, cells were stained with antibodies against Tollip and vimentin. Arrows indicate aggresomes surrounded by vimentin cage in Neuro2a cells. Alternatively, after treatment of Neuro2a cells with 10 μM nocodazole and 0.5 μM MG-132 for 12 h, cells were analyzed by immunostaining. Tollip exhibited multiple, small and granular distribution in the cytoplasm after nocodazole treatment. Bar = 20 μm. (B) Western blot analysis of soluble (sup) and insoluble (ppt) fractions prepared from Neuro2a cells after treatment with MG-132 for 24 h or untreated as a control. Blotted proteins were analyzed with indicated antibodies.

Tollip is required for maintaining cell viability against the toxicity of misfolded proteins, probably by recruiting them to aggresomes.

The formation of intracellular ubiquitinated aggregates is a hallmark of polyQ diseases including HD. Transcription factors, molecular chaperones and ubiquitin–proteasome system proteins are known to associate with the polyQ aggregates and implicated in the pathogenesis of polyQ disease [18]. However, role of aggregation in the toxicity is controversial, because accumulating evidence suggests that controlled aggregation into inclusion bodies has cell protective roles against misfolded proteins including polyQ-expanded proteins [16,17]. Tollip is involved in two major cascades of cellular functions. Firstly, Tollip interacts with the TIR domain of the IL-1R [4]. Since the TIR domain mediates the binding of the serine/threonine kinase IRAK-1 to the activated receptor complex, Tollip acts as a regulator of the signaling cascade. Secondly, Tollip is known to interact with polyubiquitinated proteins through the CUE domain and is involved in the ubiquitin–proteasome system. In the case of IL-1R, the CUE domain and TIR interacting domain of Tollip are required for endosome-mediated lysosomal degradation of IL-1R [3]. In the present study, we analyzed the role of Tollip in htt^{pQ} aggregation and cytotoxicity and found that Tollip associates with the htt^{pQ} aggregates and protect cells against htt^{pQ} toxicity by stimulating aggregation (Figs. 1 and 2).

Tollip is a multifunctional protein that interacts with a number of ubiquitin-related proteins and sumolylated proteins, and forms a complex with TOM1, polyubiquitin chains and clathrin heavy chain [9]. As Tollip localizes in endosomes [3], Tollip can function as a molecular link between endosomal processing and ubiquitin–proteasome system. In the present study, we demonstrate that Tollip colocalizes with a late endosome marker in htt^{pQ} aggregates and the aggresome formed under proteasome inhibition

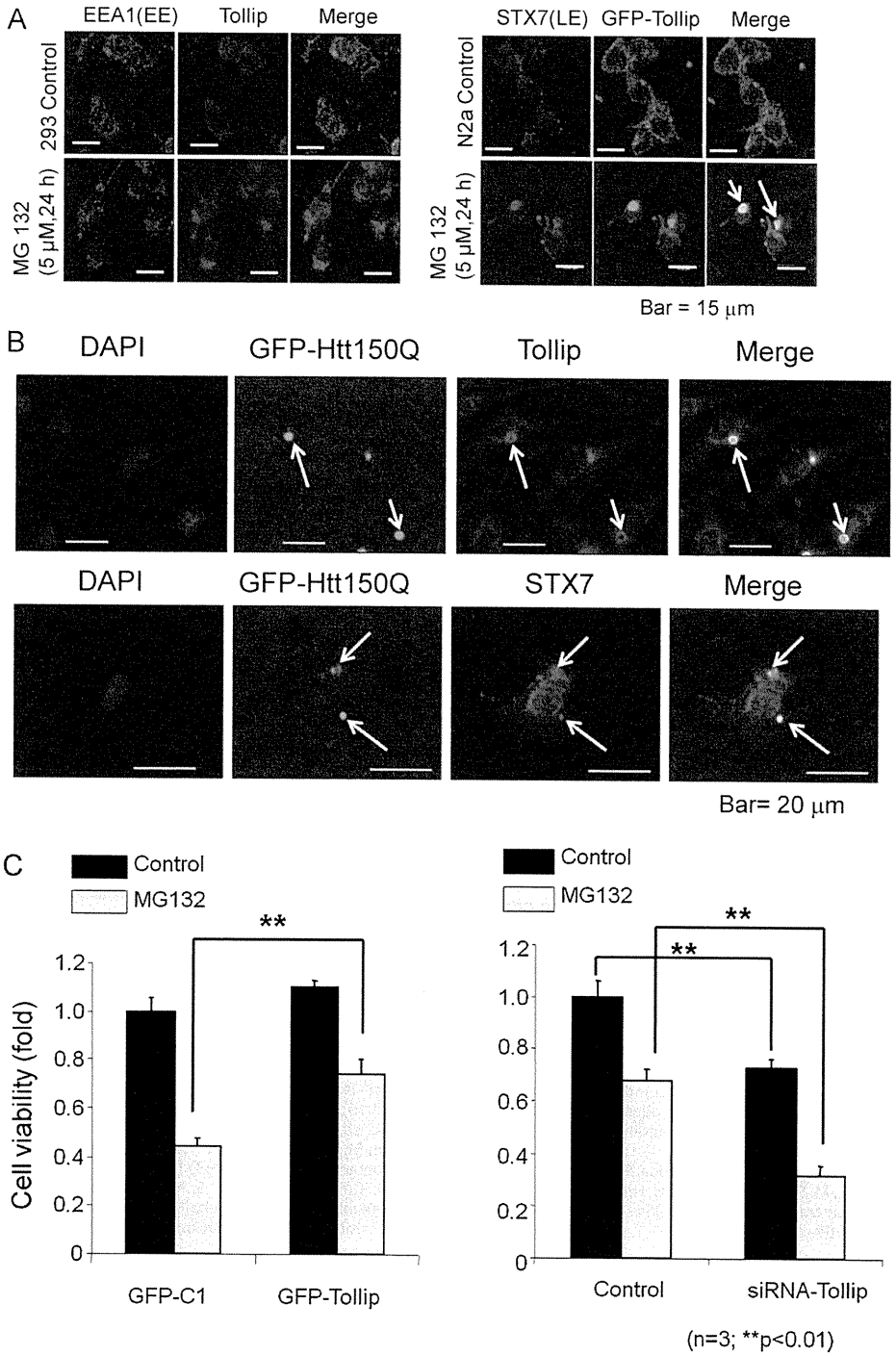

Fig. 4. Colocalization of Tollip with a late endosomal maker in MG132-induced aggresomes and htt^{pQ} inclusions and Tollip-dependent cell protection against the toxicity of proteasome inhibition. (A) HEK293 cells were co-stained with antibodies against EEA1 (early endosome marker) and Tollip (left), or GFP-Tollip transfected Neuro2a cells were stained with antibody against syntaxin-7 (late endosome marker) (right). Arrows indicate the co-localization of Tollip with syntaxin-7. Bar = 15 μm. (B) A Neuro2a cell line stably expressing GFP-htt150Q was stained with anti-Tollip (upper) or anti-syntaxin-7 (lower) antibodies. Arrows indicate the co-localization of Tollip and syntaxin-7 in htt aggregates. Bar = 20 μm. (C) After the treatment with 5 μM MG-132 for 24 h, Neuro2a cells were transiently transfected with GFP-Tollip or GFP vector as a control (left). Alternatively, cells were treated with *Tollip* siRNA or control siRNA as a control (right). Cells were then differentiated in the presence of 5 mM dbcAMP. Cell viability was measured by Titer Blue assay (Promega) ($n = 3$). **, $p < 0.001$. The difference of control cell viability between left and right panels is considered to be due to the difference in toxic effect between plasmid DNA transfection and small RNA transfection [11].

conditions (Figs. 3 and 4). These observations strongly suggest that Tollip mediates trafficking of ubiquitinated aberrant proteins to aggresomes *via* late endosomes or structures containing endosomal proteins.

Accumulating evidence indicates that ubiquitin binding proteins play crucial roles in degradation of polyQ proteins through ubiquitin and autophagy systems. For example, the ubiquitin binding protein p62 co-localizes with many types of polyubiquitinated

protein aggregates and recruit the autophagosomal protein LC3 [2]. The p62 protein recognizes polyubiquitin by the carboxyl-terminal UBA domain and is polymerized through the amino-terminal PB1 domain. Expression of p62 is strongly induced by exposure to proteasomal inhibitors or overexpression of polyglutamine-expanded proteins [18], and this protein is required for autophagic clearance of misfolded proteins [2,11,12]. Ubiquilin, another ubiquitin binding protein, protects cells against the toxicity of htt exon-1 (74Q) through authophagy [19]. Formation of inclusions/aggresomes is considered to reduce toxic misfolded species like oligomers, and ubiquitin interacting proteins may stimulate formation of aggresomes to accelerate clearance of the toxic species by microtubule-dependent controlled aggregation and degradation through the autophagy–lysosome pathway [11,14]. These observations suggest that Tollip protects cells perhaps by enhancing controlled aggregation to the aggresome using the ubiquitin binding CUE domain and the ability to interact with multiple proteins (e.g., clathrin and Tom1). Since Tollip is involved in protein transport *via* endosomes [9] and Tollip colocalized with an endosome maker in aggresomes/inclusions in our experiments, Tollip may accerelate aggregation of ubiquitinated proteins *via* endosomes, although precise roles of Tollip in the aggregation of ubiquitinated proteins and protection against misfolded proteins remain to be investigated. In conclusion, our present data indicate that Tollip is a cell protective ubiquitin binding protein that stimulates aggresome/inclusion formation in neuronal cells.

Acknowledgements

We thank Dr. Nobuyuki Nukina (RIKEN Brain Institute) for kindly providing htt expressing cell lines and helpful discussion. We also thank Drs. Takashi Tsuboi (University of Tokyo) for providing helpful ideas, Kouta Kanno (University of Tokyo) for helping htt plasmid preparation and Brent Bill (UCLA) for giving helpful advice. AO was supported by a fellowship from Japan Society for Promotion of Science.

References

[1] The Huntington's Disease Collaborative Research Group, A novel gene containing a trinucleotide repeat that is expanded and unstable on Huntington's disease chromosomes, Cell 72 (1993) 971–983.
[2] G. Bjorkoy, T. Lamark, A. Brech, H. Outzen, M. Perander, A. Overvatn, H. Stenmark, T. Johansen, p62/SQSTM1 forms protein aggregates degraded by autophagy and has a protective effect on huntingtin-induced cell death, J. Cell Biol. 171 (2005) 603–614.
[3] B. Brissoni, L. Agostini, M. Kropf, F. Martinon, V. Swoboda, S. Lippens, H. Everett, N. Aebi, S. Janssens, E. Meylan, M. Felberbaum-Corti, H. Hirling, J. Gruenberg, J. Tschopp, K. Burns, Intracellular trafficking of interleukin-1 receptor I requires Tollip, Curr. Biol. 16 (2006) 2265–2270.
[4] K. Burns, J. Clatworthy, L. Martin, F. Martinon, C. Plumpton, B. Maschera, A. Lewis, K. Ray, J. Tschopp, F. Volpe, Tollip a new component of the IL-1RI pathway, links IRAK to the IL-1 receptor, Nat. Cell Biol. 2 (2000) 346–351.
[5] H. Doi, K. Mitsui, M. Kurosawa, Y. Machida, Y. Kuroiwa, N. Nukina, Identification of ubiquitin-interacting proteins in purified polyglutamine aggregates, FEBS Lett. 571 (2004) 171–176.
[6] R. Heir, C. Ablasou, E. Dumontier, M. Elliott, C. Fagotto-Kaufmann, F.K. Bedford, The UBL domain of PLIC-1 regulates aggresome formation, EMBO Rep. 7 (2006) 1252–1258.
[7] N.R. Jana, N. Nukina, BAG-1 associates with the polyglutamine-expanded huntingtin aggregates, Neurosci. Lett. 378 (2005) 171–175.
[8] N.R. Jana, E.A. Zemskov, G. Wang, N. Nukina, Altered proteasomal function due to the expression of polyglutamine-expanded truncated N-terminal huntingtin induces apoptosis by caspase activation through mitochondrial cytochrome c release, Hum. Mol. Genet. 10 (2001) 1049–1059.
[9] Y. Katoh, Y. Shiba, H. Mitsuhashi, Y. Yanagida, H. Takatsu, K. Nakayama, Tollip and Tom1 form a complex and recruit ubiquitin-conjugated proteins onto early endosomes, J. Biol. Chem. 279 (2004) 24435–24443.
[10] A. Kitamura, H. Kubota, C.G. Pack, G. Matsumoto, S. Hirayama, Y. Takahashi, H. Kimura, M. Kinjo, R.I. Morimoto, K. Nagata, Cytosolic chaperonin prevents polyglutamine toxicity with altering the aggregation state, Nat. Cell Biol. 8 (2006) 1163–1170.
[11] M. Komatsu, Y. Ichimura, Physiological significance of selective degradation of p62 by autophagy, FEBS Lett. 584 (2010) 1374–1378.
[12] M. Komatsu, H. Kurokawa, S. Waguri, K. Taguchi, A. Kobayashi, Y. Ichimura, Y.S. Sou, I. Ueno, A. Sakamoto, K.I. Tong, M. Kim, Y. Nishito, S. Iemura, T. Natsume, T. Ueno, E. Kominami, H. Motohashi, K. Tanaka, M. Yamamoto, The selective autophagy substrate p62 activates the stress responsive transcription factor Nrf2 through inactivation of Keap1, Nat. Cell Biol. 12 (2010) 213–223.
[13] M. Komatsu, S. Waguri, M. Koike, Y.S. Sou, T. Ueno, T. Hara, N. Mizushima, J. Iwata, J. Ezaki, S. Murata, J. Hamazaki, Y. Nishito, S. Iemura, T. Natsume, T. Yanagawa, J. Uwayama, E. Warabi, H. Yoshida, T. Ishii, A. Kobayashi, M. Yamamoto, Z. Yue, Y. Uchiyama, E. Kominami, K. Tanaka, Homeostatic levels of p62 control cytoplasmic inclusion body formation in autophagy-deficient mice, Cell 131 (2007) 1149–1163.
[14] R.R. Kopito, Aggresomes, inclusion bodies and protein aggregation, Trends Cell Biol. 10 (2000) 524–530.
[15] Y.L. Lo, A.G. Beckhouse, S.L. Boulus, C.A. Wells, Diversification of TOLLIP isoforms in mouse and man, Mamm. Genome 20 (2009) 305–314.
[16] R. Luthi-Carter, D.M. Taylor, J. Pallos, E. Lambert, A. Amore, A. Parker, H. Moffitt, D.L. Smith, H. Runne, O. Gokce, A. Kuhn, Z. Xiang, M.M. Maxwell, S.A. Reeves, G.P. Bates, C. Neri, L.M. Thompson, J.L. Marsh, A.G. Kazantsev, SIRT2 inhibition achieves neuroprotection by decreasing sterol biosynthesis, Proc. Natl. Acad. Sci. U.S.A. 107 (2010) 7927–7932.
[17] R.I. Morimoto, Proteotoxic stress and inducible chaperone networks in neurodegenerative disease and aging, Genes Dev. 22 (2008) 1427–1438.
[18] U. Nagaoka, K. Kim, N.R. Jana, H. Doi, M. Maruyama, K. Mitsui, F. Oyama, N. Nukina, Increased expression of p62 in expanded polyglutamine-expressing cells and its association with polyglutamine inclusions, J. Neurochem. 91 (2004) 57–68.
[19] C. Rothenberg, D. Srinivasan, L. Mah, S. Kaushik, C.M. Peterhoff, J. Ugolino, S. Fang, A.M. Cuervo, R.A. Nixon, M.J. Monteiro, Ubiquilin functions in autophagy and is degraded by chaperone-mediated autophagy, Hum. Mol. Genet. 19 (2010) 3219–3232.
[20] S.C. Shih, G. Prag, S.A. Francis, M.A. Sutanto, J.H. Hurley, L. Hicke, A ubiquitin-binding motif required for intramolecular monoubiquitylation, the CUE domain, EMBO J. 22 (2003) 1273–1281.
[21] M. Tanaka, Y. Machida, S. Niu, T. Ikeda, N.R. Jana, H. Doi, M. Kurosawa, M. Nekooki, N. Nukina, Trehalose alleviates polyglutamine-mediated pathology in a mouse model of Huntington disease, Nat. Med. 10 (2004) 148–154.

Journal of Human Genetics (2012), 1–2

www.nature.com/jhg

CORRESPONDENCE

Myotonic dystrophy type 2 is rare in the Japanese population

Journal of Human Genetics advance online publication, 19 January 2012; doi:10.1038/jhg.2011.152

Myotonic dystrophy (DM) is the most common form of adult-onset muscular dystrophy and is characterized by autosomal dominant progressive myopathy, myotonia and multiorgan involvement. There are two distinct entities currently known: DM type 1 (DM1) and type 2 (DM2). DM2 is caused by the expansion of a tetranucleotide CCTG repeat in the first intron of the zinc finger protein 9 (*ZNF9*) gene on chromosome 3q21,[1] whereas DM1 is caused by a CTG repeat expansion in the 3′-untranslated region of the dystrophia myotonica-protein kinase gene (*DMPK*).[2] In the normal allele for *ZNF9*, the repeat sequence is a complex motif with an overall configuration of $(TG)_n(TCTG)_n(CCTG)_n$. The number of CCTG repeats is <30 in the normal allele, with interruptions by GCTG and/or TCTG motifs, and this allele is stably transmitted from one generation to the next.[1,3] However, in the expanded allele only the CCTG tract elongates and no GCTG and TCTG interruptions occur. The expanded *ZNF9* allele is extremely unstable and the size is highly variable, ranging from 75 to 11 000 repeats, with a mean of 5000 CCTG repeats. This unprecedented repeat size and somatic heterogeneity make the molecular diagnosis of DM2 difficult, and explain why the expansion yields variable clinical phenotypes.[4]

To date, DM2 mutations have been identified predominantly in European Caucasians.[3,5] Although a small number of DM2 mutations have been reported in non-European populations, including families in Morocco, Algeria, Lebanon, Afghanistan and Sri Lanka,[6,7] all reported that DM2 patients had been considered to originate from a single common founder because they shared an identical haplotype.[3,5,7] However, in 2008 we identified the first case of DM2 in an East-Asian population, in a Japanese patient with a disease haplotype distinct from that shared among Caucasians, indicating that DM2 exists in non-Caucasian populations and that there may have been separate founders.[8]

Thus, it was of interest to determine the frequency of DM2 in non-Caucasian populations. We studied a Japanese population for the presence of the DM2 mutation. We included both patients with clinically and/or electrically confirmed myotonia in which the DM1 mutation had been excluded and patients with the limb-girdle muscular dystrophy (LGMD) phenotype, because DM2 is generally proximal dominant[4] and the phenotype often lacks myotonia,[9] similar to LGMD, a heterogenous group of muscle disorders for which >60% of the genetic causes have remained undisclosed in Japan (Y.K. Hayashi *et al.*, unpublished data). It has been currently reported that the frequency of the DM2 mutation is more than DM1 in the European population:[10] 1 in 1830 in the general Finnish population, 1 in 988 Finnish patients with non-myotonic neuromuscular diseases and 1 in 93 Italian patients with undetermined non-myotonic proximal myopathy or asymptomatic hyperCKemia. Both the Finnish and Italian population are expected to be a relatively representative European population with regard to the DM2 mutation, because of a single European founder haplotype.[3,5,7]

Genomic DNA was extracted from blood leukocytes or muscle biopsy samples according to the standard protocols. The CCTG repeat size was determined by PCR, using primers flanking the repeat. When a single allele was amplified, Southern blot analysis using *Eco*RI or repeat-primed PCR specific for the DM2 expansion[1,4] was performed to distinguish homozygosity from heterozygosity involving a large CCTG expansion. All subjects included in this study gave informed consent and the protocol was approved by the Ethical Committee of Okayama University, Nagoya University and the National Center of Neurology and Psychiatry. In total, we studied 153 unrelated patients. In all, 34 were myotonic patients without the DM1 mutation and 119 showed a LGMD phenotype without identified LGMD mutations. Clinical

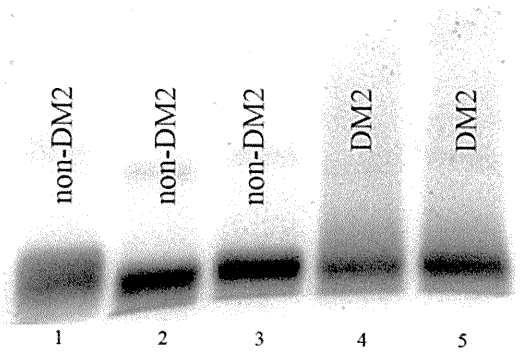

Figure 1 Repeat-primed PCR analysis. Expanded CCTG repeats in the two DM2 patients (Caucasian and Japanese DM2[9] in lanes 4 and 5, respectively) are detected as a continuous characteristic smear of products at higher molecular weight than those in non-DM2 patients (3 different individuals from the 11 patients showing a single allele by PCR amplification of the DM2 repeat in lanes 1–3).

information was assessed based on records provided by the physicians.

We identified 295 alleles ranging in length from 180 to 258 bp by PCR amplification of the DM2 repeat. Heterozygosity was identified in 142 individuals (0.93). In the remaining 11 samples showing a single allele, Southern blot or repeat-primed PCR analysis showed no expanded CCTG repeats (Figure 1), indicating that all of them are homozygous for a single allele. Thus, in our extensive survey, no DM2-related CCTG expansion was detected.

Most DM patients in Japan have been considered to have DM1 (NIH Genetics Home Reference, http://ghr.nlm.nih.gov/condition/myotonic-dystrophy). Our study confirms that DM2 is an extremely rare cause of myotonic and/or LGMD patients in Japan. Although the spectrum of clinical presentation of DM2 is variable and only one Japanese DM2 patient has been reported to date, our data have important implications concerning the indications for genetic testing and counseling for DM2 in East-Asian populations. The origin of most DM2 mutations is estimated to be 200–540 generations ago in Europe, and DM2 has since spread into several European populations.[3] The rarity of DM2 in East-Asian populations may be because of a lack of founder effects or extinction of DM2 by genetic drift or selective causes.

CONFLICT OF INTEREST

The authors declare no conflict of interest.

ACKNOWLEDGEMENTS

We appreciate the cooperation of all patients and doctors who participated in this investigation. This study was supported by Grants-in-Aid for Scientific Research from the Ministry of Education, Culture, Sports, Science and Technology, as well as Research Grants for Intractable Diseases from the Ministry of Health, Labour and Welfare, Japan (TM, KO, KA, YKH, IN).

Tohru Matsuura[1,2], Narihiro Minami[3], Hajime Arahata[3,4], Kinji Ohno[2], Koji Abe[1], Yukiko K Hayashi[3] and Ichizo Nishino[3]

[1]Department of Neurology, Okayama University Graduate School of Medicine, Dentistry and Pharmaceutical Sciences, Okayama, Japan; [2]Division of Neurogenetics, Center for Neurological Diseases and Cancer, Nagoya University Graduate School of Medicine, Nagoya, Japan; [3]Department of Neuromuscular Research, National Institute of Neuroscience, National Center of Neurology and Psychiatry, Kodaira, Tokyo, Japan and [4]Neuro-Muscular Center, National Oomuta Hospital, Fukuoka, Japan
E-mail: tohrum@cc.okayama-u.ac.jp

1 Liquori, C. L., Ricker, K., Moseley, M. L., Jacobsen, J. F., Kress, W ., Naylor, S. L. *et al.* Myotonic dystrophy type 2 caused by a CCTG expansion in intron 1 of ZNF9. *Science* **293,** 864–867 (2001).
2 Harper, P. S. in *Myotonic Dystrophy* (W.B. Saunders, London, 2001).
3 Liquori, C. L., Ikeda, Y ., Weatherspoon, M., Ricker, K., Schoser, B. G., Dalton, J. C. *et al.* Myotonic dystrophy type 2: human founder haplotype and evolutionary conservation of the repeat tract. *Am. J. Hum. Genet.* **73,** 849–862 (2003).
4 Day, J. W., Ricker, K., Jacobsen, J. F., Rasmussen, L. J., Dick, K. A., Kress, W. *et al.* Myotonic dystrophy type 2: molecular, diagnostic and clinical spectrum. *Neurology* **60,** 657–664 (2003).
5 Bachinski, L. L., Udd, B., Meola, G., Sansone, V., Bassez, G., Eymard, B. *et al.* Confirmation of the type 2 myotonic dystrophy $(CCTG)_n$ expansion mutation in patients with proximal myotonic myopathy/proximal myotonic dystrophy of different European origins: a single shared haplotype indicates an ancestral founder effect. *Am. J. Hum. Genet.* **73,** 835–848 (2003).
6 Udd, B., Meola, G., Krahe, R., Thornton, C., Ranum, L., Day, J. *et al.* Report of the 115th ENMC workshop: DM2/PROMM and other myotonic dystrophies: 3rd Workshop. *Neuromuscul. Disord.* **13,** 589–596 (2003).
7 Coenen, M. J., Tieleman, A. A., Schijvenaars, M. M., Leferink, M., Ranum, L. P., Scheffer, H. *et al.* Dutch myotonic dystrophy type 2 patients and a North-African DM2 family carry the common European founder haplotype. *Eur. J. Hum. Genet.* **19,** 567–570 (2011).
8 Saito, T., Amakusa, Y., Kimura, T., Yahara, O., Aizawa, H., Ikeda, Y. *et al.* Myotonic dystrophy type 2 in Japan: ancestral origin distinct from Caucasian families. *Neurogenetics* **9,** 61–63 (2008).
9 Young, N. P., Daube, J. R., Sorenson, E. J. & Milone, M. Absent, unrecognized, and minimal myotonic discharges in myotonic dystrophy type 2. *Muscle Nerve* **41,** 758–762 (2010).
10 Suominen, T., Bachinski, L. L., Auvinen, S., Hackman, P., Baggerly, K. A., Angelini, C. *et al.* Population frequency of myotonic dystrophy: higher than expected frequency of myotonic dystrophy type 2 (DM2) mutation in Finland. *Eur. J. Hum. Genet.* **19,** 776–782 (2011).

Expansion of Intronic GGCCTG Hexanucleotide Repeat in *NOP56* Causes SCA36, a Type of Spinocerebellar Ataxia Accompanied by Motor Neuron Involvement

Hatasu Kobayashi,[1,4] Koji Abe,[2,4] Tohru Matsuura,[2,4] Yoshio Ikeda,[2] Toshiaki Hitomi,[1] Yuji Akechi,[2] Toshiyuki Habu,[3] Wanyang Liu,[1] Hiroko Okuda,[1] and Akio Koizumi[1,*]

Autosomal-dominant spinocerebellar ataxias (SCAs) are a heterogeneous group of neurodegenerative disorders. In this study, we performed genetic analysis of a unique form of SCA (SCA36) that is accompanied by motor neuron involvement. Genome-wide linkage analysis and subsequent fine mapping for three unrelated Japanese families in a cohort of SCA cases, in whom molecular diagnosis had never been performed, mapped the disease locus to the region of a 1.8 Mb stretch (LOD score of 4.60) on 20p13 (D20S906–D20S193) harboring 37 genes with definitive open reading frames. We sequenced 33 of these and observed a large expansion of an intronic GGCCTG hexanucleotide repeat in *NOP56* and an unregistered missense variant (Phe265Leu) in *C20orf194*, but we found no mutations in *PDYN* and *TGM6*. The expansion showed complete segregation with the SCA phenotype in family studies, whereas Phe265Leu in *C20orf194* did not. Screening of the expansions in the SCA cohort cases revealed four additional occurrences, but none were revealed in the cohort of 27 Alzheimer disease cases, 154 amyotrophic lateral sclerosis cases, or 300 controls. In total, nine unrelated cases were found in 251 cohort SCA patients (3.6%). A founder haplotype was confirmed in these cases. RNA foci formation was detected in lymphoblastoid cells from affected subjects by fluorescence in situ hybridization. Double staining and gel-shift assay showed that (GGCCUG)n binds the RNA-binding protein SRSF2 but that $(CUG)_6$ does not. In addition, transcription of *MIR1292*, a neighboring miRNA, was significantly decreased in lymphoblastoid cells of SCA patients. Our finding suggests that SCA36 is caused by hexanucleotide repeat expansions through RNA gain of function.

Autosomal-dominant spinocerebellar ataxias (SCAs) are a heterogeneous group of neurodegenerative disorders characterized by loss of balance, progressive gait, and limb ataxia.[1–3] We recently encountered two unrelated patients with intriguing clinical symptoms from a community in the Chugoku region in western mainland Japan.[4] These patients both showed complicated clinical features, with ataxia as the first symptom, followed by characteristic late-onset involvement of the motor neuron system that caused symptoms similar to those of amyotrophic lateral sclerosis (ALS [MIM 105400]).[4] Some SCAs (SCA1 [MIM 164400], SCA2 [MIM 183090], SCA3 [MIM 607047], and SCA6 [MIM 183086]) are known to slightly affect motor neurons; however, their involvement is minimal and the patients usually do not develop skeletal muscle and tongue atrophies.[4] Of particular interest is that RNA foci have been recently demonstrated in hereditary disorders caused by microsatellite repeat expansions or insertions in the noncoding regions of their gene.[5–7] The unique clinical features in these families have seldom been described in previous reports; therefore, we undertook a genetic analysis.

A similar form of SCA was observed in five Japanese cases from a cohort of 251 patients with SCA, in whom molecular diagnosis had not been performed, who were followed by the Department of Neurology, Okayama University Hospital. These five cases originated from a city of 450,000 people in the Chugoku region. Thus, we suspected the presence of a founder mutation common to these five cases, prompting us to recruit these five families (pedigrees 1–5) (Figure 1, Table 1). This study was approved by the Ethics Committee of Kyoto University and the Okayama University institutional review board. Written informed consent was obtained from all subjects. An index of cases per family was investigated in some depth: IV-4 in pedigree 1, II-1 in pedigree 2, III-1 in pedigree 3, II-1 in pedigree 4, and II-1 in pedigree 5. The mean age at onset of cerebellar ataxia was 52.8 ± 4.3 years, and the disease was transmitted by an autosomal-dominant mode of inheritance. All affected individuals started their ataxic symptoms, such as gait and truncal instability, ataxic dysarthria, and uncoordinated limbs, in their late forties to fifties. MRI revealed relatively confined and mild cerebellar atrophy (Figure 2A). Unlike individuals with previously known SCAs, all affected individuals with longer disease duration showed obvious signs of motor neuron involvement (Table 1). Characteristically, all affected individuals exhibited tongue atrophy with fasciculation, although its degree of severity varied (Figure 2B). Despite severe tongue atrophy in some cases, their swallowing function was relatively preserved, and they were allowed oral intake even at a later point after onset. In addition to tongue atrophy, skeletal muscle atrophy and fasciculation in the limbs and trunk appeared in advanced cases.[4] Tendon reflexes were generally mildly to severely hyperreactive in most

[1]Department of Health and Environmental Sciences, Graduate School of Medicine, Kyoto University, Kyoto, Japan; [2]Department of Neurology, Graduate School of Medicine, Dentistry and Pharmaceutical Science, Okayama University, Okayama, Japan; [3]Radiation Biology Center, Kyoto University, Kyoto, Japan
[4]These authors contributed equally to this work
*Correspondence: koizumi.akio.5v@kyoto-u.ac.jp
DOI 10.1016/j.ajhg.2011.05.015.

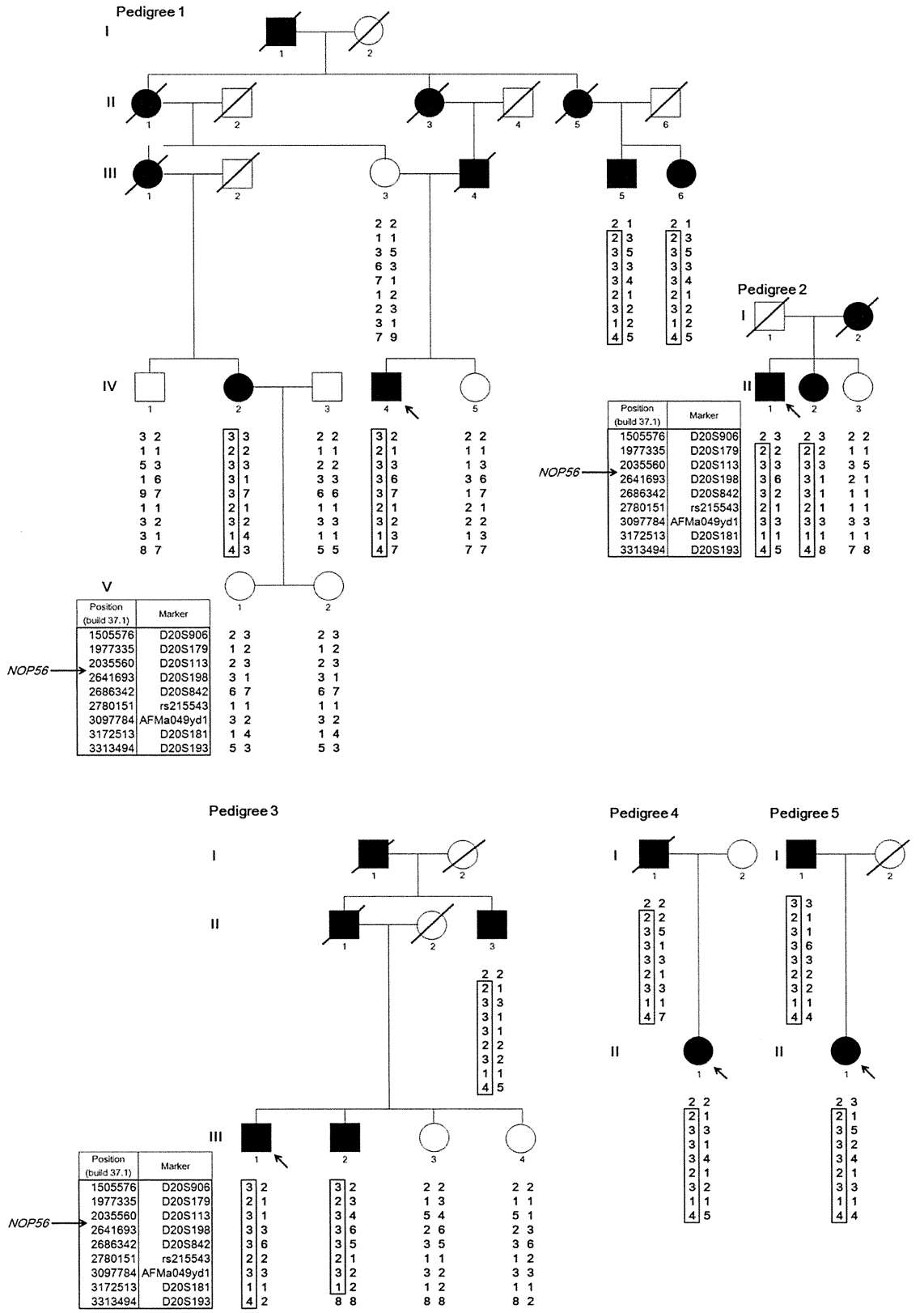

Figure 1. Pedigree Charts of the Five SCA Families
Haplotypes are shown for nine markers from D20S906 (1,505,576 bp) to D20S193 (3,313,494 bp), spanning 1.8 Mb on chromosome 20p13. *NOP56* is located at 2,633,254–2,639,039 bp (NCBI build 37.1). Filled and unfilled symbols indicate affected and unaffected individuals, respectively. Squares and circles represent males and females, respectively. A slash indicates a deceased individual. The putative founder haplotypes among patients are shown in boxes constructed by GENHUNTER.[8] Arrows indicate the index case. The pedigrees were slightly modified for privacy protection.